# UNIFIED PRINCIPLES FOR MULTI-SOURCE TRANSFER LEARNING UNDER LABEL SHIFTS

**Anonymous authors**
Paper under double-blind review

## ABSTRACT

We study the label shift problem in multi-source transfer learning and derive new generic principles to control the target generalization risk. Our theoretical backed framework unifies the principles of conditional feature alignment, label distribution ratio estimation and domain relation weights estimation. Moreover, the inspired practice provides a unified algorithm for various multi-source label shift transfer scenarios: learning with limited target data, unsupervised domain adaptation and label partial unsupervised domain adaptation. We evaluate the proposed method on these scenarios by extensive experiments and show that our proposed algorithm can significantly outperform the baselines.

## 1 INTRODUCTION

Transfer learning (Pan & Yang, 2009) is based on the motivation that learning a new task is easier after having learned several similar tasks. By learning the inductive bias from a set of related source domains $(\mathcal{S}_1, \dots, \mathcal{S}_T)$ and then leveraging the shared knowledge upon learning the target domain $\mathcal{T}$, the prediction performance can be significantly improved. Based on this, transfer learning arises in deep learning applications such as computer vision (Zhang et al., 2019; Tan et al., 2018; Hoffman et al., 2018b), natural language processing (Ruder et al., 2019; Houlsby et al., 2019) and biomedical engineering (Raghu et al., 2019; Lundervold & Lundervold, 2019; Zhang & An, 2017).

To ensure a reliable transfer, it is critical to understand the theoretical assumptions between the domains. One implicit assumption in most transfer learning algorithms is that the label proportions remain unchanged across different domains (Du Plessis & Sugiyama, 2014) (i.e., $\mathcal{S}(y) = \mathcal{T}(y)$). However, in many real-world applications, the label distributions can vary markedly (i.e. label shift) (Wen et al., 2014; Lipton et al., 2018; Li et al., 2019b), in which existing approaches cannot guarantee a small target generalization error. Moreover, transfer learning becomes more challenging when transferring knowledge from *multiple sources* to build a model for the target domain, as this requires an effective selection and leveraging the most useful source domains when label shift occurs. This is not only theoretically interesting but also commonly encountered in real-world applications. For example, in medical diagnostics, the disease distribution changes over countries (Liu et al., 2004; Geiss et al., 2014). Considering the task of diagnosing a disease in a country without sufficient data, how can we leverage the information from different countries with abundant data to help the diagnosing? Obviously, naïvely combining all the sources and applying one-to-one single source transfer learning algorithm can lead to undesired results, as it can include low quality or even untrusted data from certain sources, which can severely influence the performance.

In this paper, we study the label shift problem in multi-source transfer learning where $\mathcal{S}_t(y) \neq \mathcal{T}(y)$. We derive *unified principles* that are applicable for different scenarios: unsupervised Domain Adaptation (DA) (Ben-David et al., 2010; Li et al., 2018b), limited target labels (Mansour et al., 2020) and partial unsupervised DA with $\text{supp}(\mathcal{T}(y)) \subseteq \text{supp}(\mathcal{S}_t(y))$ (Cao et al., 2018), where prior works generally only focus on one specific scenario. It should be noted that this work deals with target shift *without* assuming that conditional distributions are identical (i.e., $\mathcal{S}_t(x|y) \neq \mathcal{T}(x|y)$), which is more realistic for real-world problems. Our contributions in this paper are two-folds:

(**I**) We propose to use Wasserstein distance (Arjovsky et al., 2017) to develop a new target generalization risk upper bound (Theorem 1), which reveals the importance of label distribution ratio estimation and provides a principled guideline to learn the domain relation coefficients. Moreover, we provide a theoretical analysis in the context of representation learning (Theorem 2), which guides

to learn a feature function that minimizes the conditional Wasserstein distance as well as controls the weighted source risk. We further reveal the relations in the aforementioned three scenarios lie in the *different assumptions* for estimating label distribution ratio. (**II**) Inspired by the theoretical results, we propose *Wasserstein Aggregation Domain Network* (WADN), a unified algorithm for multi-source transfer learning. We evaluate our algorithm on three benchmark datasets, and the results show that our algorithm can significantly outperform state-of-the-art principled approaches.

## 2 TRANSFER RISK UPPER BOUND

We assume a scoring hypothesis defined on the input space $\mathcal{X}$ and output space $\mathcal{Y}$ with $h : \mathcal{X} \times \mathcal{Y} \to \mathbb{R}$, is $K$-Lipschitz w.r.t. the feature $x$ (given the same label), i.e. for $\forall y$, $\|h(x_1, y) - h(x_2, y)\|_2 \leq K\|x_1 - x_2\|_2$, and the loss function $\ell : \mathbb{R} \times \mathbb{R} \to \mathbb{R}_+$ is positive, $L$-Lipschitz and upper bounded by $L_{\max}$. We denote the expected risk w.r.t distribution $\mathcal{D}$: $R_{\mathcal{D}}(h) = \mathbb{E}_{(x,y)\sim\mathcal{D}}\ell(h(x, y))$ and its empirical counterpart (w.r.t. $\hat{\mathcal{D}}$) $\hat{R}_{\mathcal{D}}(h) = \sum_{(x,y)\in\hat{\mathcal{D}}} \ell(h(x, y))$. Based on previous works, the label shift is generally handled by label-distribution ratio weighted loss: $R^{\alpha}_{\mathcal{S}}(h) = \mathbb{E}_{(x,y)\sim\mathcal{S}}\alpha(y)\ell(h(x, y))$ with $\alpha_t(y) = \mathcal{T}(y)/\mathcal{S}(y)$. We also denote $\hat{\alpha}_t$ as its empirical counterpart, estimated from samples. Besides, to measure the task relations, we define a simplex $\boldsymbol{\lambda}$ ($\boldsymbol{\lambda}[t] \geq 0, \sum_{t=1}^{T} \boldsymbol{\lambda}[t] = 1$) as the task relation coefficient vector.

We first present Theorem 1, which indicates how $\hat{\alpha}_t$ and $\boldsymbol{\lambda}$ affect the target risk.

**Theorem 1.** *Let $\{\hat{\mathcal{S}}_t = \{(x_i, y_i)\}_{i=1}^{N_{\mathcal{S}_t}}\}_{t=1}^{T}$ and $\hat{\mathcal{T}} = \{(x_i, y_i)\}_{i=1}^{N_{\mathcal{T}}}$, respectively be $T$ source and target i.i.d. samples. For $\forall h \in \mathcal{H}$ with $\mathcal{H}$ the hypothesis family and $\forall\boldsymbol{\lambda}$, with high probability $\geq 1 - 4\delta$, the target risk can be upper bounded by:*

$$R_{\mathcal{T}}(h) \leq \sum_t \boldsymbol{\lambda}[t]\hat{R}^{\hat{\alpha}_t}_{\mathcal{S}_t}(h) + LK\sum_t \boldsymbol{\lambda}[t]\mathbb{E}_{y\sim\hat{\mathcal{T}}(y)}W_1(\hat{\mathcal{T}}(x|Y = y)\|\hat{\mathcal{S}}_t(x|Y = y)) + L_{\max}d^{\sup}_{\infty}\sqrt{\sum_{t=1}^{T}\frac{\boldsymbol{\lambda}[t]^2}{\beta_t}}\sqrt{\frac{\log(1/\delta)}{2N}}$$
$$+ L_{\max}\sup_t \|\alpha_t - \hat{\alpha}_t\|_2 + \mathit{Comp}(N_{\mathcal{S}_1}, \ldots, N_{\mathcal{S}_T}, N_{\mathcal{T}}, \delta),$$

*where $N = \sum_{t=1}^{T} N_{\mathcal{S}_t}$ and $\beta_t = N_{\mathcal{S}_t}/N$ and $d^{\sup}_{\infty} = \max_{t\in[1,T],y\in[1,\mathcal{Y}]} \alpha_t(y)$ the maximum true label distribution ratio value. $W_1(\cdot\|\cdot)$ is the Wasserstein-1 distance with $L_2$-distance as cost function. Comp$(N_{\mathcal{S}_1}, \ldots, N_{\mathcal{S}_T}, N_{\mathcal{T}}, \delta)$ is a function that decreases with larger $N_{\mathcal{S}_1}, \ldots, N_{\mathcal{T}}$, given a fixed $\delta$ and hypothesis family $\mathcal{H}$. (See Appendix D for details)*

**Remarks** (I) The upper bound is controlled by $\hat{\alpha}_t$ with $\hat{\alpha}_t$-weighted loss and $\|\hat{\alpha}_t - \alpha_t\|_2$ (the gap between ground-truth and empirical label ratio). Therefore if we can estimate a good $\hat{\alpha}_t$ and minimize re-weighted loss, these terms can be small. If target labels are available, $\hat{\alpha}_t$ can be directly computed from the observed data and $\hat{\alpha}_t \to \alpha_t$. If target labels are absent (unsupervised DA), we need to design methods to estimate $\hat{\alpha}_t$ (Sec. 3). (II) The upper bound is also related with $\boldsymbol{\lambda}$. To minimize this upper bound, we need to assign a higher $\boldsymbol{\lambda}[t]$ to the source $t$ with a *smaller weighted prediction loss* and *a smaller weighted conditional Wasserstein distance*. Intriguingly, $\sqrt{\sum_{t=1}^{T} \boldsymbol{\lambda}^2[t]/\beta_t}$ plays as a regularization term of $\boldsymbol{\lambda}$ for avoiding concentrating only one single source domain but tends to the uniform assignment. (III) Comp$(N_{\mathcal{S}_1}, \ldots, N_{\mathcal{S}_T}, N_{\mathcal{T}}, \delta)$ is a function that reflects the convergence behavior, which decreases with larger observation numbers. If we fix $\mathcal{H}, \delta$, $N$ and $N_{\mathcal{T}}$, this term can be viewed as a constant.

**Insights in Representation Learning** Apart from Theorem 1, we propose a theoretical analysis in the context of *representation learning*, which motivates practical guidelines in the deep learning regime. We define a stochastic feature function $g$ and we denote its conditional distribution w.r.t. latent variable $Z$ (induced by $g$) as $\mathcal{S}(z|Y = y) = \int_x g(z|x)\mathcal{S}(x|Y = y)dx$. Then we have:

**Theorem 2.** *We assume the settings of loss, the hypothesis are the same with Theorem 1. We further denote the stochastic feature learning function $g : \mathcal{X} \to \mathcal{Z}$, and the hypothesis $h : \mathcal{Z} \times \mathcal{Y} \to \mathbb{R}$. Then $\forall\boldsymbol{\lambda}$, the target risk is upper bounded by:*

$$R_{\mathcal{T}}(h, g) \leq \sum_t \boldsymbol{\lambda}[t]R^{\alpha_t}_{\mathcal{S}_t}(h, g) + LK\sum_t \boldsymbol{\lambda}[t]\mathbb{E}_{y\sim\mathcal{T}(y)}W_1(\mathcal{S}_t(z|Y = y)\|\mathcal{T}(z|Y = y)),$$

*where $R_{\mathcal{T}}(h, g) = \mathbb{E}_{(x,y)\sim\mathcal{T}(x,y)}\mathbb{E}_{z\sim g(z|x)}\ell(h(z, y))$.*

Table 1: Practical principles under different scenarios

| Transfer Scenarios | Learn $(g, h)$ | Estimate $\hat{\alpha}_t$ | Estimate $\boldsymbol{\lambda}$ |
|---|---|---|---|
| Multi-Source Transfer with Limited Target Data | Sec. 3.1 | $\hat{\mathcal{T}}(y)/\hat{\mathcal{S}}_t(y)$ | Sec. 3.3 |
| Unsupervised Multi-Source DA | | Sec. 3.2 | |
| Partial Unsupervised Multi-Source DA | | | |

**Remark** Theorem 2 reveals that to control the upper bound, we need to learn $g$ that minimizes the weighted conditional Wasserstein distance and learn $(g, h)$ that minimizes the weighted source risk.

## 3 Unified Practical Framework in Deep Learning

The theoretical results in Section 2 motivate general principles to follow when designing multi-source transfer learning algorithms. We summarize those principles in the following rules.

(I) Learn a $g$ that minimizes the weighted conditional Wasserstein distance as well as learn $(g, h)$ that minimizes the $\hat{\alpha}_t$-weighted source risk (Sec. 3.1).

(II) Properly estimate the label distribution ratio $\hat{\alpha}_t$ (Sec. 3.2).

(III) Balance the trade-off between assigning a higher $\boldsymbol{\lambda}[t]$ to the source $t$ that has a smaller weighted prediction loss and conditional Wasserstein distance, and assigning balanced $\boldsymbol{\lambda}[t]$. (Sec. 3.3).

We instantiate these rules with a unified practical framework for solving multi-source transfer learning problems, as shown in Tab 1. We would like to point out that our original theoretical result is based on setting with the available target labels. *The proposed algorithm can be applied to unsupervised scenarios.*

### 3.1 Guidelines in the representation learning

Motivated by Theorem 2, given a fixed label ratio estimation $\hat{\alpha}_t$ and fixed $\boldsymbol{\lambda}$, we should find a representation function $g : \mathcal{X} \to \mathcal{Z}$ and a hypothesis function $h : \mathcal{Z} \times \mathcal{Y} \to \mathbb{R}$ such that:

$$\min_{g,h} \sum_t \boldsymbol{\lambda}[t] \hat{R}^{\hat{\alpha}_t}_{\mathcal{S}_t}(h, g) + C_0 \sum_t \boldsymbol{\lambda}[t] \mathbb{E}_{y\sim\hat{\mathcal{T}}(y)} W_1(\hat{\mathcal{S}}_t(z|Y = y) \| \hat{\mathcal{T}}(z|Y = y)) \tag{1}$$

**Explicit Conditional Loss** When target label information is available, one can *explicitly* solve the conditional optimal transport problem with $g$ and $h$ for a given $Y = y$. However, due to the high computational complexity in solving $T \times |\mathcal{Y}|$ optimal transport problems, the original form is practically intractable. To address this issue, we propose to approximate the conditional distribution on latent space $Z$ as Gaussian distribution with identical Covariance matrix such that $\hat{\mathcal{S}}_t(z|Y = y) \approx \mathcal{N}(\mathbf{C}^y_t, \boldsymbol{\Sigma})$ and $\hat{\mathcal{T}}(z|Y = y) \approx \mathcal{N}(\mathbf{C}^y, \boldsymbol{\Sigma})$. Then we have $W_1(\hat{\mathcal{S}}_t(z|Y = y) \| \hat{\mathcal{T}}(z|Y = y)) \leq \|\mathbf{C}^y_t - \mathbf{C}^y\|_2$ (see Appendix F for details). Intuitively, the approximation term is equivalent to the well known *feature mean matching* (Sugiyama & Kawanabe, 2012), which computes the feature centroid of each class (on latent space $Z$) and aligns them by minimizing their $L_2$ distance.

**Implicit Conditional Loss** When target label information is not available (e.g. unsupervised DA and partial DA), the explicit matching approach can adopt pseudo-label predicted by the hypothesis $h$ as a surrogate of the true target label. However, in the early stage of the learning process, the pseudo-labels can be unreliable, which can lead to an inaccurate estimate of $W_1(\hat{\mathcal{S}}(z|Y = y) \| \hat{\mathcal{T}}(z|Y = y))$. To address this, the following Lemma indicates that estimating the conditional Wasserstein distance is equivalent to estimating the Wasserstein adversarial loss weighted by the label-distribution ratio.

**Lemma 1.** *The weighted conditional Wasserstein distance can be implicitly expressed as:*

$$\sum_t \boldsymbol{\lambda}[t] \mathbb{E}_{y\sim\mathcal{T}(y)} W_1(\mathcal{S}_t(z|Y = y) \| \mathcal{T}(z|Y = y)) = \max_{d_1,\cdots,d_T} \sum_t \boldsymbol{\lambda}[t] [\mathbb{E}_{z\sim\mathcal{S}_t(z)} \bar{\alpha}_t(z) d_t(z) - \mathbb{E}_{z\sim\mathcal{T}(z)} d_t(z)],$$

*where* $\bar{\alpha}_t(z) = \mathbf{1}_{\{(z,y)\sim\mathcal{S}_t\}}\alpha_t(Y=y)$*, and* $d_1, \dots, d_T : \mathcal{Z} \to R_+$ *are the* 1*-Lipschitz domain discriminators (Ganin et al., 2016; Arjovsky et al., 2017).*

Lemma 1 reveals that instead of using pseudo-labels to estimate the weighted conditional Wasserstein distance, one can train $T$ domain discriminators with weighted Wasserstein adversarial loss, which does not require the pseudo-label of each target sample during the matching. On the other hand, $\bar{\alpha}_t$ can be obtained from $\hat{\alpha}_t$, which will be elaborated in Sec. 3.2.

In practice, we adopt a *hybrid* approach by linearly combining the explicit and implicit matching strategies for all the scenarios, in which empirical results show its effectiveness.

### 3.2 Estimate label distribution ratio $\hat{\alpha}_t$

**Multi-Source Transfer with target labels** When the target labels are available, $\hat{\alpha}_t$ can be directly estimated from the data without any assumption and $\hat{\alpha}_t \to \alpha_t$ can be proved from asymptotic statistics.

**Unsupervised Multi-Source DA** In this scenario, it is impossible to estimate a good $\hat{\alpha}_t$ without imposing any additional assumptions. Following (Zhang et al., 2013; Lipton et al., 2018; Azizzadenesheli et al., 2019; Combes et al., 2020), we assume that the conditional distributions are aligned between the target and source domains (i.e., $\mathcal{S}_t(z|y) = \mathcal{T}(z|y)$). Then, we denote $\bar{\mathcal{S}}_t(y)$, $\bar{\mathcal{T}}(y)$ as the predicted $t$-source/target label distribution through the hypothesis $h$, and also define $C_{\hat{\mathcal{S}}_t}[y,k] = \hat{\mathcal{S}}_t[\text{argmax}_{y'} h(z,y') = y, Y = k]$ is the $t$-source *prediction confusion matrix*. We can demonstrate that if the conditional distribution is aligned, we have $\bar{\mathcal{T}}(y) = \bar{\mathcal{T}}_{\hat{\alpha}_t}(y)$, with $\bar{\mathcal{T}}_{\hat{\alpha}_t}(Y=y) = \sum_{k=1}^{\mathcal{Y}} C_{\hat{\mathcal{S}}_t}[y,k]\hat{\alpha}_t(k)$ the constructed target prediction distribution from the $t$-source information. (See Appendix H for the proof). Then we can estimate $\hat{\alpha}_t$ through matching these two distributions by minimizing $D_{\text{KL}}(\bar{\mathcal{T}}(y)\|\bar{\mathcal{T}}_{\hat{\alpha}_t}(y))$, which is equivalent to:

$$\min_{\hat{\alpha}_t} \quad -\sum_{y=1}^{|\mathcal{Y}|} \bar{\mathcal{T}}(y) \log(\sum_{k=1}^{|\mathcal{Y}|} C_{\hat{\mathcal{S}}_t}[y,k]\hat{\alpha}_t(k)) \quad \text{s.t} \quad \forall y \in \mathcal{Y}, \hat{\alpha}_t(y) \geq 0, \quad \sum_{y=1}^{|\mathcal{Y}|} \hat{\alpha}_t(y)\hat{\mathcal{S}}_t(y) = 1 \tag{2}$$

In the aforementioned part, we have assumed the conditional distribution is aligned, which is a feasible requirement in our algorithm, since the goal of $g$ exactly aims at gradually achieving this. In the experiments, we iteratively estimate $\hat{\alpha}_t$ and learn $g$.

**Unsupervised Multi-Source Partial DA** When $\text{supp}(\mathcal{T}(y)) \subseteq \text{supp}(\mathcal{S}_t(y))$, $\alpha_t$ is sparse due to the non-overlapped classes. Accordingly, in addition to the assumption of $\mathcal{S}_t(z|y) = \mathcal{T}(z|y)$ as in unsupervised DA, we also impose such prior knowledge by adding a regularizer $\|\hat{\alpha}_t\|_1$ to the objective of Eq. (2) to induce sparsity in $\hat{\alpha}_t$ (See Appendix I for more details).

In training the neural network, since the non-overlapped classes will be automatically assigned with a small or zero $\hat{\alpha}_t$, $(g,h)$ will be less affected by the classes with small $\hat{\alpha}_t$. Our empirical results effectively validate its capability in detecting non-overlapping classes and show significant improvements over other baselines.

### 3.3 Estimate task relation coefficient $\lambda$

Inspired by Theorem 1, given *fixed* $\hat{\alpha}_t$ and $(g,h)$, we estimate $\boldsymbol{\lambda}$ through optimizing the derived upper bound.

$$\begin{aligned} \min_{\boldsymbol{\lambda}} \quad & \sum_t \boldsymbol{\lambda}[t]\hat{R}^{\hat{\alpha}_t}_{\mathcal{S}_t}(h,g) + C_0 \sum_t \boldsymbol{\lambda}[t]\mathbb{E}_{y\sim\hat{\mathcal{T}}(y)} W_1(\hat{\mathcal{T}}(z|Y=y)\|\hat{\mathcal{S}}(z|Y=y)) + C_1\sqrt{\sum_{t=1}^{T}\frac{\boldsymbol{\lambda}^2[t]}{\beta_t}} \\ \text{s.t} \quad & \forall t, \boldsymbol{\lambda}[t] \geq 0, \sum_{t=1}^{T}\boldsymbol{\lambda}[t] = 1 \end{aligned} \tag{3}$$

In practice, $\hat{R}^{\hat{\alpha}_t}_{\mathcal{S}_t}(h,g)$ is the weighted empirical prediction error and $\mathbb{E}_{y\sim\hat{\mathcal{T}}(y)} W_1(\hat{\mathcal{T}}(z|Y=y)\|\hat{\mathcal{S}}(z|Y=y))$ is approximated by the dynamic feature centroid distance $\sum_y \bar{\mathcal{T}}(y)\|\mathbf{C}^y_t - \mathbf{C}^y\|_2$ (See Appendix K for details). Thus, solving $\boldsymbol{\lambda}$ is a standard convex optimization problem.

### 3.4 ALGORITHM DESCRIPTION

Based on the aforementioned components, we present a brief description of WADN (Algorithm 1) in the unsupervised scenarios (UDA and Partial DA), which iteratively updates $(g, h)$, $\hat{\alpha}_t$, and $\boldsymbol{\lambda}$. As for the the detailed descriptions and WADN under target label information, we refer to Appendix K.

**Algorithm 1** Wasserstein Aggregation Domain Network (unsupervised scenario, one iteration)

**Ensure:** Label ratio $\hat{\alpha}_t$ and task relation $\boldsymbol{\lambda}$. Feature Learner $g$, Classifier $h$, statistic critic function $d_1, \ldots, d_T$, class centroid for source $\mathbf{C}_t^y$ and target $\mathbf{C}^y$ ($\forall t = [1, T], y \in \mathcal{Y}$).

1: $\triangleright \triangleright \triangleright$ DNN Parameter Training Stage (fixed $\alpha_t$ and $\boldsymbol{\lambda}$) $\triangleleft \triangleleft \triangleleft$

2: **for** mini-batch of samples $(\mathbf{x}_{\mathcal{S}_1}, \mathbf{y}_{\mathcal{S}_1}) \sim \hat{\mathcal{S}}_1, \ldots, (\mathbf{x}_{\mathcal{S}_T}, \mathbf{y}_{\mathcal{S}_T}) \sim \hat{\mathcal{S}}_T$, $(\mathbf{x}_{\mathcal{T}}) \sim \hat{\mathcal{T}}$ **do**

3: Predict target pseudo-label $\bar{\mathbf{y}}_{\mathcal{T}} = \text{argmax}_y h(g(\mathbf{x}_{\mathcal{T}}), y)$

4: Compute unnormalized source confusion matrix on current *batch* $C_{\hat{\mathcal{S}}_t}[y, k]$ $(t = 1, \ldots, T)$

5: Compute feature centroid for source $C_t^y$ and target $C^y$ on current *batch*; Use moving average to update source and target class centroid $\mathbf{C}_t^y$ and $\mathbf{C}^y$.

6: Updating $g, h, d_1, \ldots, d_T$ (SGD), by optimizing:

$$\min_{g,h} \max_{d_1,\ldots,d_T} \underbrace{\sum_t \boldsymbol{\lambda}[t] \hat{R}_{\mathcal{S}_t}^{\hat{\alpha}_t}(h, g)}_{\text{Classification Loss}} + \epsilon C_0 \underbrace{\sum_t \boldsymbol{\lambda}[t] \mathbb{E}_{y \sim \bar{\mathcal{T}}(y)} \|\mathbf{C}_t^y - \mathbf{C}^y\|_2}_{\text{Explicit Conditional Loss}} + (1-\epsilon) C_0 \underbrace{\sum_t \boldsymbol{\lambda}[t] [\mathbb{E}_{z \sim \hat{\mathcal{S}}_t(z)} \bar{\alpha}_t(z) d(z) - \mathbb{E}_{z \sim \hat{\mathcal{T}}(z)} d(z)]}_{\text{Implicit Conditional Loss}}$$

7: **end for**

8: $\triangleright \triangleright \triangleright$ Estimation $\hat{\alpha}_t$ and $\boldsymbol{\lambda}$ $\triangleleft \triangleleft \triangleleft$

9: Compute normalized source confusion matrix; Solve $\{\hat{\alpha}_t\}_{t=1}^T$ w.r.t. current training epoch (Sec. 3.2 Unsupervised DA or Partial DA); Update global $\hat{\alpha}_t$ through moving average.

10: Solve $\boldsymbol{\lambda}$ (Sec. 3.3) w.r.t. current training epoch; Update global $\boldsymbol{\lambda}$ through moving average.

## 4 RELATED WORK

Due to the space limit, we refer to Appendix A for the related work, which covers theory and algorithm of multi-source transfer learning; label shift; label-partial transfer learning and scenarios that relate to multi-source transfer problems.

## 5 EXPERIMENTS

In this section, we compare proposed approaches with several baselines for the popular tasks. For all the scenarios, the following baselines are evaluated: (I) **Source** method applied only labelled source data to train the model. (II) **DANN** (Ganin et al., 2016). We follow the protocol of Wen et al. (2020) to merge all the source dataset as a global source domain. (III) **MDAN** (Zhao et al., 2018); (IV) **MDMN** (Li et al., 2018b); (V) **M$^3$SDA** (Peng et al., 2019) adopted maximizing classifier discrepancy (Saito et al., 2018) and (VI) **DARN** (Wen et al., 2020). For the conventional multi-source transfer and partial unsupervised multi-source DA, we additionally compare specific baselines. All the baselines are re-implemented in the same network structure for fair comparisons. The detailed network structures, hyper-parameter settings, training details are put in Appendix L.

We evaluate the performance on three different datasets: (I) **Amazon Review.** (Blitzer et al., 2007) It contains four domains (Books, DVD, Electronics, and Kitchen) with positive and negative product reviews. We follow the common data pre-processing strategies as (Chen et al. (2012)) to form a 5000-dimensional bag-of-words feature. Note that the label distribution in the original dataset is uniform. *To enhance the benefits of the proposed approach, we create a label distribution drifted task by randomly dropping* $50\%$ *negative reviews of all the sources while keeping the target identical.* (show in Fig.3 (a)). (II) **Digits**. It consists four digits recognition datasets including MNIST, USPS (Hull, 1994), SVHN (Netzer et al., 2011) and Synth (Ganin et al., 2016). *We also create a slight label distribution drift for the sources by randomly dropping* $50\%$ *samples on digits 5-9 and keep target identical.* (showed in Fig.(3)(b)). (III) **Office-Home Dataset** (Venkateswara et al., 2017). It contains 65 classes for four different domains: Art, Clipart, Product and Real-World. We used the ResNet50 (He et al., 2016) pretrained from the ImageNet in PyTorch as the base network for

feature learning and put a MLP for the classification. The label distributions in these four domains are different and we did not manually create a label drift (showed in Fig.3 (c)).

### 5.1 UNSUPERVISED MULTI-SOURCE DA

In the unsupervised multi-source DA, we evaluate the proposed approach on all the three datasets. We use a similar hyper-parameter selection strategy as in DANN (Ganin et al., 2016). All reported results are averaged from five runs. The detailed experimental settings are illustrated in Appendix L. The empirical results are illustrated in Tab. 2, 3 and 4. Since we did not change the target label distribution throughout the whole experiments, then we still use the target accuracy as the metric. We report the means and standard deviations for each approach. The best approaches based on a two-sided Wilcoxon signed-rank test (significance level $p = 0.05$) are shown in bold.

Table 2: Unsupervised DA: Accuracy $(\%)$ on Source-Shifted Amazon Review.

| Target | Books | DVD | Electronics | Kitchen | Average |
|---|---|---|---|---|---|
| Source | $68.15_{\pm 1.37}$ | $69.51_{\pm 0.74}$ | $82.09_{\pm 0.88}$ | $75.30_{\pm 1.29}$ | 73.81 |
| DANN | $65.59_{\pm 1.35}$ | $67.23_{\pm 0.71}$ | $80.49_{\pm 1.11}$ | $74.71_{\pm 1.53}$ | 72.00 |
| MDAN | $68.77_{\pm 2.31}$ | $67.81_{\pm 2.46}$ | $80.96_{\pm 0.77}$ | $75.67_{\pm 1.96}$ | 73.30 |
| MDMN | $70.56_{\pm 1.05}$ | $69.64_{\pm 0.73}$ | $82.71_{\pm 0.71}$ | $77.05_{\pm 0.78}$ | 74.99 |
| $M^3$SDA | $69.09_{\pm 1.26}$ | $68.67_{\pm 1.37}$ | $81.34_{\pm 0.66}$ | $76.10_{\pm 1.47}$ | 73.79 |
| DARN | $71.21_{\pm 1.16}$ | $68.68_{\pm 1.12}$ | $81.51_{\pm 0.81}$ | $77.71_{\pm 1.09}$ | 74.78 |
| WADN | $\mathbf{73.72}_{\pm 0.63}$ | $\mathbf{79.64}_{\pm 0.34}$ | $\mathbf{84.64}_{\pm 0.48}$ | $\mathbf{83.73}_{\pm 0.50}$ | **80.43** |

Table 3: Unsupervised DA: Accuracy $(\%)$ on the Source-Shifted Digits.

| Target | MNIST | SVHN | SYNTH | USPS | Average |
|---|---|---|---|---|---|
| Source | $84.93_{\pm 1.50}$ | $67.14_{\pm 1.40}$ | $78.11_{\pm 1.31}$ | $86.02_{\pm 1.12}$ | 79.05 |
| DANN | $86.99_{\pm 1.53}$ | $69.56_{\pm 2.26}$ | $78.73_{\pm 1.30}$ | $86.81_{\pm 1.74}$ | 80.52 |
| MDAN | $87.86_{\pm 2.24}$ | $69.13_{\pm 1.56}$ | $79.77_{\pm 1.69}$ | $86.50_{\pm 1.59}$ | 80.81 |
| MDMN | $87.31_{\pm 1.88}$ | $69.84_{\pm 1.59}$ | $80.27_{\pm 0.88}$ | $86.61_{\pm 1.41}$ | 81.00 |
| $M^3$SDA | $87.22_{\pm 1.70}$ | $68.89_{\pm 1.93}$ | $80.01_{\pm 1.77}$ | $86.39_{\pm 1.68}$ | 80.87 |
| DARN | $86.98_{\pm 1.29}$ | $68.59_{\pm 1.79}$ | $80.68_{\pm 0.61}$ | $86.85_{\pm 1.78}$ | 80.78 |
| WADN | $\mathbf{89.07}_{\pm 0.72}$ | $\mathbf{71.66}_{\pm 0.77}$ | $\mathbf{82.06}_{\pm 0.89}$ | $\mathbf{90.07}_{\pm 1.10}$ | **83.22** |

Table 4: Unsupervised DA: Accuracy $(\%)$ on Office-Home

| Target | Art | Clipart | Product | Real-World | Average |
|---|---|---|---|---|---|
| Source | $49.25_{\pm 0.60}$ | $46.89_{\pm 0.61}$ | $66.54_{\pm 1.72}$ | $73.64_{\pm 0.91}$ | 59.08 |
| DANN | $50.32_{\pm 0.32}$ | $50.11_{\pm 1.16}$ | $68.18_{\pm 1.27}$ | $73.71_{\pm 1.63}$ | 60.58 |
| MDAN | $67.93_{\pm 0.36}$ | $66.61_{\pm 1.32}$ | $79.24_{\pm 1.52}$ | $81.82_{\pm 0.65}$ | 73.90 |
| MDMN | $68.38_{\pm 0.58}$ | $67.42_{\pm 0.53}$ | $82.49_{\pm 0.56}$ | $83.32_{\pm 1.93}$ | 75.28 |
| $M^3$SDA | $63.77_{\pm 1.07}$ | $62.30_{\pm 0.44}$ | $75.85_{\pm 1.24}$ | $79.92_{\pm 0.60}$ | 70.46 |
| DARN | $69.89_{\pm 0.42}$ | $68.61_{\pm 0.50}$ | $83.37_{\pm 0.62}$ | $84.29_{\pm 0.46}$ | 76.54 |
| WADN | $\mathbf{73.78}_{\pm 0.43}$ | $\mathbf{70.18}_{\pm 0.54}$ | $\mathbf{86.32}_{\pm 0.38}$ | $\mathbf{87.28}_{\pm 0.87}$ | **79.39** |

The empirical results reveal a significantly better performance ($\approx 3\%$) on different datasets. For understanding the working principles of WADN, we evaluate the performance under different levels of source label shift in Amazon Review dataset (Fig.1(a)). The results show strong practical benefits for WADN during a gradual larger label shift. In addition, we visualize the task relations in digits (Fig.1(b)) and demonstrate a *non-uniform* $\boldsymbol{\lambda}$, which highlights the importance of properly choosing the most related source rather than simply merging all the data. E.g. when the target domain is SVHN, WADN mainly leverages the information from SYNTH, since they are more semantically similar and MNIST does not help too much for SVHN (observed by Ganin et al. (2016)). The additional analysis and results can be found in Appendix M.

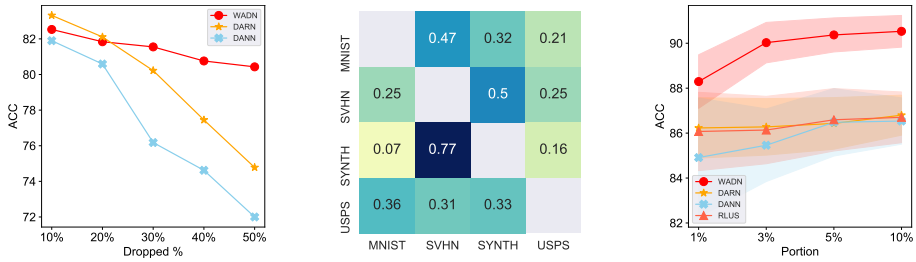


(a) (b) (c)

Figure 1: (a) Unsupervised DA with Amazon Review dataset. Accuracy under different levels of shifted sources (higher dropping rate means larger label shift). The results are averaged on all target domains. See the results for each task in Fig. (11). (b) Visualization of $\boldsymbol{\lambda}$ in unsupervised DA, each row corresponds to one target domain. (c) Transfer learning with limited target labels in USPS. The performance of WADN is consistently better under different target samples (smaller portion indicates fewer target samples).

### 5.2 Multi-Source Transfer Learning with Limited Target Samples

We adopt Amazon Review and Digits in the multi-source transfer learning with limited target samples, which have been widely used. In the experiments, we still use shifted sources. We randomly sample only $10\%$ labeled samples (w.r.t. target dataset in unsupervised DA) as training set and the rest $90\%$ samples as the unseen target test set. (See Appendix L for details). We adopt the same hyper-parameters and training strategies with unsupervised DA. We specifically add a recent baseline RLUS (Konstantinov & Lampert, 2019), which also considered multi-source transfer learning with the labeled target.

Table 5: Multi-source Transfer: Accuracy $(\%)$ on Source-Shifted Amazon Review

| Target | Books | DVD | Electronics | Kitchen | Average |
|---|---|---|---|---|---|
| Source + Tar | $72.59_{\pm 1.89}$ | $73.02_{\pm 1.84}$ | $81.59_{\pm 1.58}$ | $77.03_{\pm 1.73}$ | 76.06 |
| DANN | $67.35_{\pm 2.28}$ | $66.33_{\pm 2.42}$ | $78.03_{\pm 1.72}$ | $74.31_{\pm 1.71}$ | 71.50 |
| MDAN | $68.70_{\pm 2.99}$ | $69.30_{\pm 2.21}$ | $78.78_{\pm 2.21}$ | $74.07_{\pm 1.89}$ | 72.71 |
| MDMN | $69.19_{\pm 2.09}$ | $68.71_{\pm 2.39}$ | $81.88_{\pm 1.46}$ | $78.51_{\pm 1.91}$ | 74.57 |
| $M^3$SDA | $69.28_{\pm 1.78}$ | $67.40_{\pm 0.46}$ | $76.28_{\pm 0.81}$ | $76.50_{\pm 1.19}$ | 72.36 |
| DARN | $68.57_{\pm 1.35}$ | $68.77_{\pm 1.81}$ | $80.19_{\pm 1.66}$ | $77.51_{\pm 1.20}$ | 73.76 |
| RLUS | $71.83_{\pm 1.71}$ | $69.64_{\pm 2.39}$ | $81.98_{\pm 1.04}$ | $78.69_{\pm 1.15}$ | 75.54 |
| WADN | $\mathbf{74.83}_{\pm 0.84}$ | $\mathbf{75.05}_{\pm 0.62}$ | $\mathbf{84.23}_{\pm 0.58}$ | $\mathbf{81.53}_{\pm 0.90}$ | **78.91** |

Table 6: Multi-source Transfer: Accuracy $(\%)$ on the Source-Shifted Digits

| Target | MNIST | SVHN | SYNTH | USPS | Average |
|---|---|---|---|---|---|
| Source + Tar | $79.63_{\pm 1.74}$ | $56.48_{\pm 1.90}$ | $69.64_{\pm 1.38}$ | $86.29_{\pm 1.56}$ | 73.01 |
| DANN | $86.77_{\pm 1.30}$ | $69.13_{\pm 1.09}$ | $78.82_{\pm 1.35}$ | $86.54_{\pm 1.03}$ | 80.32 |
| MDAN | $86.93_{\pm 1.05}$ | $68.25_{\pm 1.53}$ | $79.80_{\pm 1.17}$ | $86.23_{\pm 1.41}$ | 80.30 |
| MDMN | $77.59_{\pm 1.36}$ | $69.62_{\pm 1.26}$ | $78.93_{\pm 1.64}$ | $87.26_{\pm 1.13}$ | 78.35 |
| $M^3$SDA | $85.88_{\pm 2.06}$ | $68.84_{\pm 1.05}$ | $76.29_{\pm 0.95}$ | $87.15_{\pm 1.10}$ | 79.54 |
| DARN | $86.58_{\pm 1.46}$ | $68.86_{\pm 1.30}$ | $80.47_{\pm 0.67}$ | $86.80_{\pm 0.89}$ | 80.68 |
| RLUS | $87.61_{\pm 1.08}$ | $\mathbf{70.50}_{\pm 0.94}$ | $79.52_{\pm 1.30}$ | $86.70_{\pm 1.13}$ | 81.08 |
| WADN | $\mathbf{88.32}_{\pm 1.17}$ | $\mathbf{70.64}_{\pm 1.02}$ | $\mathbf{81.53}_{\pm 1.11}$ | $\mathbf{90.53}_{\pm 0.71}$ | **82.75** |

The results are reported in Tabs. 5, 6, which also indicates strong empirical benefits. To show the effectiveness of WADN, we select various portions of labelled samples ($1\% \sim 10\%$) on the target. The results in Fig.1(c) on USPS dataset shows a consistently better than the baselines, even in the few target samples.

### 5.3 PARTIAL UNSUPERVISED MULTI-SOURCE DA

In this scenario, we adopt the Office-Home dataset to evaluate our approach, as it contains large (65) classes. We do not change the source domains and we randomly choose 35 classes from the target. We evaluate all the baselines on the same selected classes and repeat 5 times. All reported results are averaged from 3 different sub-class selections (15 runs in total), showing in Tab.7. (See Appendix L for details.) We additionally compare PADA (Cao et al., 2018) approach by merging all the sources and use *one-to-one* partial DA algorithm. We adopt the same hyper-parameters and training strategies with unsupervised DA scenario.

Table 7: Unsupervised Partial DA: Accuracy (%) on Office-Home (#Source: 65, #Target: 35)

| Target | Art | Clipart | Product | Real-World | Average |
|---|---|---|---|---|---|
| Source | $50.56_{\pm 1.42}$ | $49.79_{\pm 1.14}$ | $68.10_{\pm 1.33}$ | $78.24_{\pm 0.76}$ | 61.67 |
| DANN | $53.86_{\pm 2.23}$ | $52.71_{\pm 2.20}$ | $71.25_{\pm 2.44}$ | $76.92_{\pm 1.21}$ | 63.69 |
| MDAN | $67.56_{\pm 1.39}$ | $65.38_{\pm 1.30}$ | $81.49_{\pm 1.92}$ | $83.44_{\pm 1.01}$ | 74.47 |
| MDMN | $68.13_{\pm 1.08}$ | $65.27_{\pm 1.93}$ | $81.33_{\pm 1.29}$ | $84.00_{\pm 0.64}$ | 74.68 |
| $M^3$SDA | $65.10_{\pm 1.97}$ | $61.80_{\pm 1.99}$ | $76.19_{\pm 2.44}$ | $79.14_{\pm 1.51}$ | 70.56 |
| DARN | $71.53_{\pm 0.63}$ | $69.31_{\pm 1.08}$ | $82.87_{\pm 1.56}$ | $84.76_{\pm 0.57}$ | 77.12 |
| PADA | $74.37_{\pm 0.84}$ | $69.64_{\pm 0.80}$ | $83.45_{\pm 1.13}$ | $85.64_{\pm 0.39}$ | 78.28 |
| WADN | $\mathbf{80.06}_{\pm 0.93}$ | $\mathbf{75.90}_{\pm 1.06}$ | $\mathbf{89.55}_{\pm 0.72}$ | $\mathbf{90.40}_{\pm 0.39}$ | **83.98** |

The reported results are also significantly better than the current multi-source DA or one-to-one partial DA approach, which verifies the benefits of WADN: properly estimating $\hat{\alpha}_t$ and assigning proper $\boldsymbol{\lambda}$ for each source.

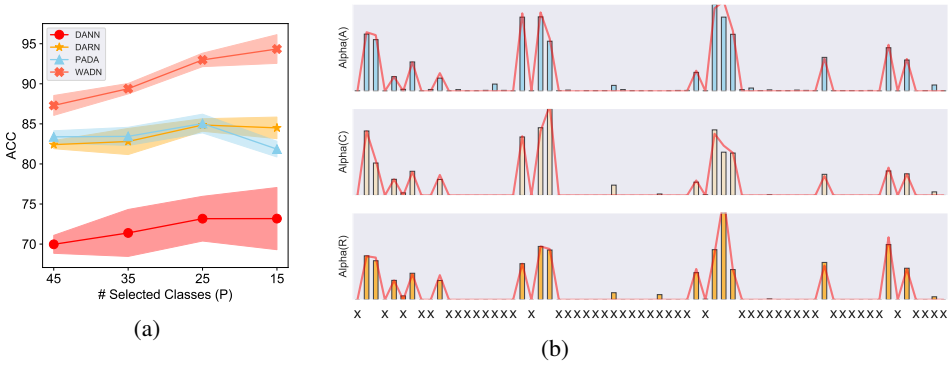


(a) (b)

Figure 2: Analysis on Partial DA of target Product. (a) Performance (mean $\pm$ std) of different selected classes on the target; (b) We select 15 classes and visualize estimated $\hat{\alpha}_t$ (the bar plot). The "X" along the x-axis represents the index of *dropped* 50 classes. The red curves are the true label distribution ratio. See Appendix N for additional results and analysis.

Besides, we change the number of selected classes (Fig 2(a)), the proposed WADN still indicates consistent better results by a large margin, which indicates the importance of considering $\hat{\alpha}_t$ and $\boldsymbol{\lambda}$. In contrast, DANN shows unstable results in less selected classes. (See Appendix N for details) Beside, WADN shows a good estimation of the label distribution ratio (Fig 2(b)) and has correctly detected the non-overlapping classes, which indicates its good explainability.

## 6 CONCLUSION

In this paper, we proposed a new theoretical principled algorithm WADN (Wasserstein Aggregation Domain Network) to solve the multi-source transfer learning problem under target shift. WADN provides a unified solution for various deep multi-source transfer scenarios: learning with limited target data, unsupervised DA, and partial unsupervised DA. We evaluate the proposed method by extensive experiments and show its strong empirical results.

## REFERENCES


Kei Akuzawa, Yusuke Iwasawa, and Yutaka Matsuo. Adversarial invariant feature learning with accuracy constraint for domain generalization. In *Joint European Conference on Machine Learning and Knowledge Discovery in Databases*, pp. 315–331. Springer, 2019.

Martin Arjovsky, Soumith Chintala, and Léon Bottou. Wasserstein gan. *arXiv preprint arXiv:1701.07875*, 2017.

Kamyar Azizzadenesheli, Anqi Liu, Fanny Yang, and Animashree Anandkumar. Regularized learning for domain adaptation under label shifts. In *International Conference on Learning Representations*, 2019. URL `https://openreview.net/forum?id=rJl0r3R9KX`.

Shai Ben-David, John Blitzer, Koby Crammer, Alex Kulesza, Fernando Pereira, and Jennifer Wortman Vaughan. A theory of learning from different domains. *Machine learning*, 79(1-2):151–175, 2010.

John Blitzer, Mark Dredze, and Fernando Pereira. Biographies, bollywood, boom-boxes and blenders: Domain adaptation for sentiment classification. In *Proceedings of the 45th annual meeting of the association of computational linguistics*, pp. 440–447, 2007.

Silvia Bucci, Antonio D'Innocente, and Tatiana Tommasi. Tackling partial domain adaptation with self-supervision. In *International Conference on Image Analysis and Processing*, pp. 70–81. Springer, 2019.

Zhangjie Cao, Lijia Ma, Mingsheng Long, and Jianmin Wang. Partial adversarial domain adaptation. In *Proceedings of the European Conference on Computer Vision (ECCV)*, pp. 135–150, 2018.

Zhangjie Cao, Kaichao You, Mingsheng Long, Jianmin Wang, and Qiang Yang. Learning to transfer examples for partial domain adaptation. In *Proceedings of the IEEE Conference on Computer Vision and Pattern Recognition*, pp. 2985–2994, 2019.

Minmin Chen, Zhixiang Xu, Kilian Q Weinberger, and Fei Sha. Marginalized denoising autoencoders for domain adaptation. In *Proceedings of the 29th International Coference on International Conference on Machine Learning*, pp. 1627–1634, 2012.

Xilun Chen, Ahmed Hassan Awadallah, Hany Hassan, Wei Wang, and Claire Cardie. Multi-source cross-lingual model transfer: Learning what to share. In *Proceedings of the 57th Annual Meeting of the Association for Computational Linguistics*, 2019.

Zhihong Chen, Chao Chen, Zhaowei Cheng, Ke Fang, and Xinyu Jin. Selective transfer with reinforced transfer network for partial domain adaptation. In *AAAI Conference on Artificial Intelligence*, 2020.

Stergios Christodoulidis, Marios Anthimopoulos, Lukas Ebner, Andreas Christe, and Stavroula Mougiakakou. Multisource transfer learning with convolutional neural networks for lung pattern analysis. *IEEE journal of biomedical and health informatics*, 21(1):76–84, 2016.

Remi Tachet des Combes, Han Zhao, Yu-Xiang Wang, and Geoff Gordon. Domain adaptation with conditional distribution matching and generalized label shift. *arXiv preprint arXiv:2003.04475*, 2020.

Marthinus Christoffel Du Plessis and Masashi Sugiyama. Semi-supervised learning of class balance under class-prior change by distribution matching. *Neural Networks*, 50:110–119, 2014.

Chelsea Finn, Pieter Abbeel, and Sergey Levine. Model-agnostic meta-learning for fast adaptation of deep networks. In *ICML*, 2017.

Yaroslav Ganin, Evgeniya Ustinova, Hana Ajakan, Pascal Germain, Hugo Larochelle, François Laviolette, Mario Marchand, and Victor Lempitsky. Domain-adversarial training of neural networks. *The Journal of Machine Learning Research*, 17(1):2096–2030, 2016.

Linda S Geiss, Jing Wang, Yiling J Cheng, Theodore J Thompson, Lawrence Barker, Yanfeng Li, Ann L Albright, and Edward W Gregg. Prevalence and incidence trends for diagnosed diabetes among adults aged 20 to 79 years, united states, 1980-2012. *Jama*, 312(12):1218–1226, 2014.

Mingming Gong, Kun Zhang, Tongliang Liu, Dacheng Tao, Clark Glymour, and Bernhard Schölkopf. Domain adaptation with conditional transferable components. In *International conference on machine learning*, pp. 2839–2848, 2016.

Ishaan Gulrajani, Faruk Ahmed, Martin Arjovsky, Vincent Dumoulin, and Aaron C Courville. Improved training of wasserstein gans. In *Advances in Neural Information Processing Systems*, pp. 5767–5777, 2017.

Kaiming He, Xiangyu Zhang, Shaoqing Ren, and Jian Sun. Deep residual learning for image recognition. In *Proceedings of the IEEE conference on computer vision and pattern recognition*, pp. 770–778, 2016.

Judy Hoffman, Brian Kulis, Trevor Darrell, and Kate Saenko. Discovering latent domains for multi-source domain adaptation. In *European Conference on Computer Vision*, pp. 702–715. Springer, 2012.

Judy Hoffman, Mehryar Mohri, and Ningshan Zhang. Algorithms and theory for multiple-source adaptation. In *Advances in Neural Information Processing Systems*, pp. 8246–8256, 2018a.

Judy Hoffman, Eric Tzeng, Taesung Park, Jun-Yan Zhu, Phillip Isola, Kate Saenko, Alexei Efros, and Trevor Darrell. Cycada: Cycle-consistent adversarial domain adaptation. In *International conference on machine learning*, pp. 1989–1998. PMLR, 2018b.

Neil Houlsby, Andrei Giurgiu, Stanislaw Jastrzebski, Bruna Morrone, Quentin De Laroussilhe, Andrea Gesmundo, Mona Attariyan, and Sylvain Gelly. Parameter-efficient transfer learning for nlp. *arXiv preprint arXiv:1902.00751*, 2019.

Jonathan J. Hull. A database for handwritten text recognition research. *IEEE Transactions on pattern analysis and machine intelligence*, 16(5):550–554, 1994.

Maximilian Ilse, Jakub M Tomczak, Christos Louizos, and Max Welling. Diva: Domain invariant variational autoencoders. *arXiv preprint arXiv:1905.10427*, 2019.

Nikola Konstantinov and Christoph Lampert. Robust learning from untrusted sources. In *International Conference on Machine Learning*, pp. 3488–3498, 2019.

Joshua Lee, Prasanna Sattigeri, and Gregory Wornell. Learning new tricks from old dogs: Multi-source transfer learning from pre-trained networks. In *Advances in Neural Information Processing Systems*, pp. 4370–4380, 2019.

Jingmei Li, Weifei Wu, Di Xue, and Peng Gao. Multi-source deep transfer neural network algorithm. *Sensors*, 19(18):3992, 2019a.

Ya Li, Xinmei Tian, Mingming Gong, Yajing Liu, Tongliang Liu, Kun Zhang, and Dacheng Tao. Deep domain generalization via conditional invariant adversarial networks. In *Proceedings of the European Conference on Computer Vision (ECCV)*, pp. 624–639, 2018a.

Yitong Li, David E Carlson, et al. Extracting relationships by multi-domain matching. In *Advances in Neural Information Processing Systems*, pp. 6798–6809, 2018b.

Yitong Li, Michael Murias, Samantha Major, Geraldine Dawson, and David Carlson. On target shift in adversarial domain adaptation. In *The 22nd International Conference on Artificial Intelligence and Statistics*, pp. 616–625, 2019b.

Chuang Lin, Sicheng Zhao, Lei Meng, and Tat-Seng Chua. Multi-source domain adaptation for visual sentiment classification. *arXiv preprint arXiv:2001.03886*, 2020.

Zachary Lipton, Yu-Xiang Wang, and Alexander Smola. Detecting and correcting for label shift with black box predictors. In *International Conference on Machine Learning*, pp. 3122–3130, 2018.

Jing Liu, Yuling Hong, Ralph B D'Agostino Sr, Zhaosu Wu, Wei Wang, Jiayi Sun, Peter WF Wilson, William B Kannel, and Dong Zhao. Predictive value for the chinese population of the framingham chd risk assessment tool compared with the chinese multi-provincial cohort study. *Jama*, 291(21): 2591–2599, 2004.

Alexander Selvikvåg Lundervold and Arvid Lundervold. An overview of deep learning in medical imaging focusing on mri. *Zeitschrift für Medizinische Physik*, 29(2):102–127, 2019.

Yishay Mansour, Mehryar Mohri, and Afshin Rostamizadeh. Multiple source adaptation and the rényi divergence. In *Proceedings of the Twenty-Fifth Conference on Uncertainty in Artificial Intelligence*, pp. 367–374. AUAI Press, 2009.

Yishay Mansour, Mehryar Mohri, Ananda Theertha Suresh, and Ke Wu. A theory of multiple-source adaptation with limited target labeled data. *arXiv preprint arXiv:2007.09762*, 2020.

Mehryar Mohri and Andres Munoz Medina. New analysis and algorithm for learning with drifting distributions. In *International Conference on Algorithmic Learning Theory*, pp. 124–138. Springer, 2012.

Saeid Motiian, Marco Piccirilli, Donald A. Adjeroh, and Gianfranco Doretto. Unified deep supervised domain adaptation and generalization. In *The IEEE International Conference on Computer Vision (ICCV)*, Oct 2017.

Yuval Netzer, Tao Wang, Adam Coates, Alessandro Bissacco, Bo Wu, and Andrew Y Ng. Reading digits in natural images with unsupervised feature learning. 2011.

XuanLong Nguyen, Martin J Wainwright, Michael I Jordan, et al. On surrogate loss functions and f-divergences. *The Annals of Statistics*, 37(2):876–904, 2009.

Sinno Jialin Pan and Qiang Yang. A survey on transfer learning. *IEEE Transactions on knowledge and data engineering*, 22(10):1345–1359, 2009.

Zhongyi Pei, Zhangjie Cao, Mingsheng Long, and Jianmin Wang. Multi-adversarial domain adaptation. *arXiv preprint arXiv:1809.02176*, 2018.

Xingchao Peng, Qinxun Bai, Xide Xia, Zijun Huang, Kate Saenko, and Bo Wang. Moment matching for multi-source domain adaptation. In *Proceedings of the IEEE International Conference on Computer Vision*, pp. 1406–1415, 2019.

Maithra Raghu, Chiyuan Zhang, Jon Kleinberg, and Samy Bengio. Transfusion: Understanding transfer learning for medical imaging. In *Advances in neural information processing systems*, pp. 3347–3357, 2019.

Ievgen Redko, Nicolas Courty, Rémi Flamary, and Devis Tuia. Optimal transport for multi-source domain adaptation under target shift. In Kamalika Chaudhuri and Masashi Sugiyama (eds.), *Proceedings of Machine Learning Research*, volume 89 of *Proceedings of Machine Learning Research*, pp. 849–858. PMLR, 16–18 Apr 2019. URL `http://proceedings.mlr.press/v89/redko19a.html`.

Sebastian Ruder. An overview of multi-task learning in deep neural networks. *arXiv preprint arXiv:1706.05098*, 2017.

Sebastian Ruder, Matthew E Peters, Swabha Swayamdipta, and Thomas Wolf. Transfer learning in natural language processing. In *Proceedings of the 2019 Conference of the North American Chapter of the Association for Computational Linguistics: Tutorials*, pp. 15–18, 2019.

Kate Saenko, Brian Kulis, Mario Fritz, and Trevor Darrell. Adapting visual category models to new domains. In *European conference on computer vision*, pp. 213–226. Springer, 2010.

Kuniaki Saito, Kohei Watanabe, Yoshitaka Ushiku, and Tatsuya Harada. Maximum classifier discrepancy for unsupervised domain adaptation. In *Proceedings of the IEEE Conference on Computer Vision and Pattern Recognition*, pp. 3723–3732, 2018.

Shai Shalev-Shwartz and Shai Ben-David. *Understanding machine learning: From theory to algorithms*. Cambridge university press, 2014.

Jake Snell, Kevin Swersky, and Richard Zemel. Prototypical networks for few-shot learning. In *Advances in neural information processing systems*, pp. 4077–4087, 2017.

Petar Stojanov, Mingming Gong, Jaime G Carbonell, and Kun Zhang. Data-driven approach to multiple-source domain adaptation. *Proceedings of machine learning research*, 89:3487, 2019.

Masashi Sugiyama and Motoaki Kawanabe. *Machine learning in non-stationary environments: Introduction to covariate shift adaptation*. MIT press, 2012.

Flood Sung, Yongxin Yang, Li Zhang, Tao Xiang, Philip HS Torr, and Timothy M Hospedales. Learning to compare: Relation network for few-shot learning. In *Proceedings of the IEEE Conference on Computer Vision and Pattern Recognition*, pp. 1199–1208, 2018.

Ben Tan, Erheng Zhong, Evan Wei Xiang, and Qiang Yang. Multi-transfer: Transfer learning with multiple views and multiple sources. In *Proceedings of the 2013 SIAM International Conference on Data Mining*, pp. 243–251. SIAM, 2013.

Chuanqi Tan, Fuchun Sun, Tao Kong, Wenchang Zhang, Chao Yang, and Chunfang Liu. A survey on deep transfer learning. In *International conference on artificial neural networks*, pp. 270–279. Springer, 2018.

Hemanth Venkateswara, Jose Eusebio, Shayok Chakraborty, and Sethuraman Panchanathan. Deep hashing network for unsupervised domain adaptation. In *Proceedings of the IEEE Conference on Computer Vision and Pattern Recognition*, pp. 5018–5027, 2017.

Haotian Wang, Wenjing Yang, Zhipeng Lin, and Yue Yu. Tmda: Task-specific multi-source domain adaptation via clustering embedded adversarial training. In *2019 IEEE International Conference on Data Mining (ICDM)*, pp. 1372–1377. IEEE, 2019.

Jonathan Weed, Francis Bach, et al. Sharp asymptotic and finite-sample rates of convergence of empirical measures in wasserstein distance. *Bernoulli*, 25(4A):2620–2648, 2019.

Pengfei Wei, Ramon Sagarna, Yiping Ke, Yew-Soon Ong, and Chi-Keong Goh. Source-target similarity modelings for multi-source transfer gaussian process regression. In *International Conference on Machine Learning*, pp. 3722–3731, 2017.

Junfeng Wen, Chun-Nam Yu, and Russell Greiner. Robust learning under uncertain test distributions: Relating covariate shift to model misspecification. In *International Conference on Machine Learning*, pp. 631–639, 2014.

Junfeng Wen, Russell Greiner, and Dale Schuurmans. Domain aggregation networks for multi-source domain adaptation. *Proceedings of the 37th International Conference on Machine Learning*, 2020.

Yifan Wu, Ezra Winston, Divyansh Kaushik, and Zachary Lipton. Domain adaptation with asymmetrically-relaxed distribution alignment. In *International Conference on Machine Learning*, pp. 6872–6881, 2019.

Yi Yao and Gianfranco Doretto. Boosting for transfer learning with multiple sources. In *2010 IEEE Computer Society Conference on Computer Vision and Pattern Recognition*, pp. 1855–1862. IEEE, 2010.

Jing Zhang, Zewei Ding, Wanqing Li, and Philip Ogunbona. Importance weighted adversarial nets for partial domain adaptation. In *Proceedings of the IEEE Conference on Computer Vision and Pattern Recognition*, pp. 8156–8164, 2018.

Jing Zhang, Wanqing Li, Philip Ogunbona, and Dong Xu. Recent advances in transfer learning for cross-dataset visual recognition: A problem-oriented perspective. *ACM Computing Surveys (CSUR)*, 52(1):1–38, 2019.

Kun Zhang, Bernhard Schölkopf, Krikamol Muandet, and Zhikun Wang. Domain adaptation under target and conditional shift. In *International Conference on Machine Learning*, pp. 819–827, 2013.

YiNan Zhang and MingQiang An. Deep learning-and transfer learning-based super resolution reconstruction from single medical image. *Journal of healthcare engineering*, 2017.

Yu Zhang and Qiang Yang. A survey on multi-task learning. *arXiv preprint arXiv:1707.08114*, 2017.

Yu Zhang and Dit-Yan Yeung. A convex formulation for learning task relationships in multi-task learning. *arXiv preprint arXiv:1203.3536*, 2012.

Han Zhao, Shanghang Zhang, Guanhang Wu, José MF Moura, Joao P Costeira, and Geoffrey J Gordon. Adversarial multiple source domain adaptation. In *Advances in neural information processing systems*, pp. 8559–8570, 2018.

Sicheng Zhao, Guangzhi Wang, Shanghang Zhang, Yang Gu, Yaxian Li, Zhichao Song, Pengfei Xu, Runbo Hu, Hua Chai, and Kurt Keutzer. Multi-source distilling domain adaptation. *arXiv preprint arXiv:1911.11554*, 2019.

Sicheng Zhao, Bo Li, Pengfei Xu, and Kurt Keutzer. Multi-source domain adaptation in the deep learning era: A systematic survey. *arXiv preprint arXiv:2002.12169*, 2020.

Yongchun Zhu, Fuzhen Zhuang, and Deqing Wang. Aligning domain-specific distribution and classifier for cross-domain classification from multiple sources. In *Proceedings of the AAAI Conference on Artificial Intelligence*, volume 33, pp. 5989–5996, 2019.

# A RELATED WORK

**Multi-source transfer learning Theory** has been investigated in the previous literature. In the unsupervised DA, (Ben-David et al., 2010; Zhao et al., 2018; Peng et al., 2019) adopted $\mathcal{H}$-divergence of marginal distribution $\mathcal{D}(x)$ to estimate the domain relations. (Li et al., 2018b) also applied Wasserstein distance of $\mathcal{D}(x)$ to estimate pair-wise domain distance. Mansour et al. (2009); Wen et al. (2020) used the Discrepancy distance to derive a tighter theoretical bound. The motivated practice from the aforementioned method used the feature information to learn the task relations, which is *generally difficult to handle label shift*. In the multi-source transfer learning with target labels, Hoffman et al. (2018a) used Rényi divergence that requires $\text{supp}(\mathcal{T}(x)) \subseteq \text{supp}(\mathcal{S}(x))$, which generally does not hold in the complicated real-world applications. Konstantinov & Lampert (2019); Mansour et al. (2020) adopted $\mathcal{Y}$-discrepancy (Mohri & Medina, 2012) to measure the joint distribution similarity. However, $\mathcal{Y}$ discrepancy is practically difficult to estimate from the data. As for the theories for understanding the partial multi-source DA, to the best of our knowledge, we first propose the theoretical insights to analyze its target risk. More importantly, we propose unified theoretical principles across these three scenarios to learn the representation and reveal their inherent relations under the label shift, which remains elusive in the multi-source transfer learning literature.

**Multi-source transfer learning Practice** has been proposed from various prospective. The key idea is to estimate the importance of different sources and then select the most related ones, to mitigate the influence of negative transfer. In the multi-source unsupervised DA, (Pei et al., 2018; Zhao et al., 2019; Zhu et al., 2019; Zhao et al., 2020; 2019; Stojanov et al., 2019; Li et al., 2019b; Wang et al., 2019; Lin et al., 2020) proposed different practical strategies in the classification, regression and semantic segmentation problems. In the presence of target labels, Hoffman et al. (2012); Tan et al. (2013); Wei et al. (2017); Yao & Doretto (2010); Konstantinov & Lampert (2019) used generalized linear model to learn the target. Christodoulidis et al. (2016); Li et al. (2019a); Chen et al. (2019) focused on deep learning approaches and Lee et al. (2019) proposed an ad-hoc strategy to combine to sources in the few-shot target domains. These ideas are generally data-driven approaches and do not analyze the why the proposed practice can control the generalization error.

**Label-Shift** Label-Shift (Zhang et al., 2013; Gong et al., 2016) is a common phenomena in the distribution shift setting, where it exhibits different $\mathcal{Y}$-marginal distributions ($\mathcal{S}(y) \neq \mathcal{T}(y)$). [1] We noticed that several theoretical principled approaches have been proposed such as RLSS (Azizzadenesheli et al., 2019), which match the target prediction distribution through $L_2$ distance with a consistent estimator such that $\|\hat{\alpha}_t - \alpha_t\|_2 \to 0$. (Combes et al., 2020; Wu et al., 2019) analyzed the generalized label shift problem in the one-to-one single unsupervised DA problem. While we focus on *how to aggregate different sources* to ensure a reliable transfer, which is more challenging. (Redko et al., 2019) proposed optimal transport strategy for the multiple unsupervised DA under label shift. However they did not consider the representation learning in conjunction with their framework. Notably, estimating high dimensional terms in the original optimal transport is highly computationally expensive (as we discussed in the paper), an efficient neural network based approaches is not ensured. Different from these, we analyzed our problem in the context of representation learning and propose an efficient (approximation the upper bound or weighted adversarial training) and principled strategies. *More importantly, our theoretical results highlights the importance of label shift problem in a variety of multi-source transfer problem.* While the aforementioned work generally focus on the unsupervised DA problem, without considering a unified practice for different scenarios (such as partial multi-source DA).

**Label-Partial Transfer Learning** Label-Partial can be viewed as a special case of the label-shift. [2] Most existing works focus on one-to-one partial transfer learning (Zhang et al., 2018; Chen et al., 2020; Bucci et al., 2019; Cao et al., 2019) by adopting the re-weighting training approach without a formal understanding. In our paper, we first rigorously analyzed this common practice and adopt the label distribution ratio as its weights, which provides a principled approach in this scenario.

[1] In our paper, the term *label shift* is used emphasizing the different target distributions $\mathcal{T}(y) \neq \mathcal{S}_t(y)$. In the previous work, they generally assume identical conditional distribution with $\mathcal{S}_t(x|y) = \mathcal{T}(x|y)$. In our paper, we **do not** require this assumption. In addition, Theorem 1 explicitly expresses how different conditional distributions influence the risk upper bound.

[2] Since $\text{supp}(\mathcal{T}(y)) \subseteq \text{supp}(\mathcal{S}_t(y))$ then we naturally have $\mathcal{T}(y) \neq \mathcal{S}_t(y)$.

### A.1 OTHER SCENARIOS RELATED TO MULTI-SOURCE TRANSFER LEARNING

**Domain Generalization** The domain generalization (DG) resembles multi-source transfer but aims at different goals. A common setting in DG is to learn multiple source but directly predict on the unseen target domain. The conventional DG approaches generally learn a distribution invariant features (Saenko et al., 2010; Motiian et al., 2017; Ilse et al., 2019) or conditional distribution invariant features (Li et al., 2018a; Akuzawa et al., 2019). However, our theoretical results reveal that in the presence of label shift (i.e $\alpha_t(y) \neq 1$) and outlier tasks then learning conditional or marginal invariant features can not guarantee a small target risk. Our theoretical result enables a formal understanding about the inherent difficulty in DG problems.

**Few-Shot Learning** The few-shot learning (Finn et al., 2017; Snell et al., 2017; Sung et al., 2018) can be viewed as a very specific scenario of multi-source transfer learning. We would like to point out the differences between the few-shot learning and our paper. (1) Few-shot learning generally involves a **very large set** of source domains $T \gg 1$ and each domain consists a **modest number** of observations $N_{\mathcal{S}_t}$. In our paper, we are interested in the a **modest number** of source domains $T$ but each source domain including a **sufficient large** number of observations ($N_{\mathcal{S}_t} \gg 1$). (2) In the target domain, the few-shot setting generally used K-samples ($K$ is very small) for each class for the fine-tuning. We would like to point out this setting generally violates our theoretical assumption. In our paper, we assume the target data is i.i.d. sampled from $\mathcal{D}(x, y)$. It is equivalently viewed that we first i.i.d. sample $y \sim \mathcal{D}(y)$, then i.i.d. sample $x \sim \mathcal{D}(x|y)$. Generally the $\mathcal{D}(y)$ is **non-uniform**, thus few-shot setting are generally not applicable for our theoretical assumptions.

**Multi-Task Learning** The goal of multi-task learning (Zhang & Yang, 2017) aims to improve the prediction performance of **all** the tasks. In our paper, we aim at controlling the prediction risk of a specified target domain. We also notice some practical techniques are common such as the shared parameter (Zhang & Yeung, 2012), shared representation (Ruder, 2017), etc.

## B ADDITIONAL FIGURES RELATED TO THE MAIN PAPER

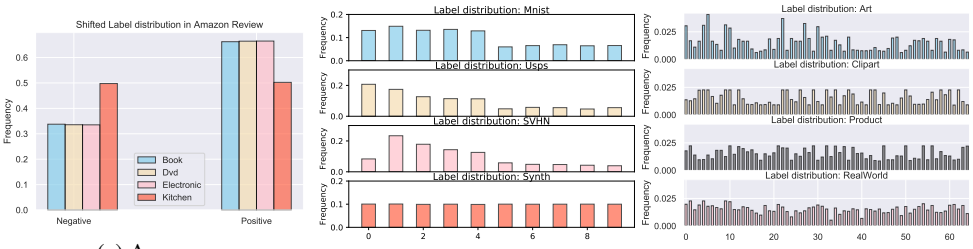


(a) Amazon (b) Digits (c) Office-Home

Figure 3: Label distribution visualization. (a) One example in Amazon Review dataset with sources: Book, Dvd, Electronic and target: Kitchen. We randomly drop $50\%$ of the negative reviews in all the sources while keeping target label distribution unchanged. (b) One example in Digits dataset with Sources: MNIST, USPS, SVHN and Target Synth. We randomly drop $50\%$ data on digits 5-9 in all sources while keeping target label distribution unchanged. (c) Office-Home dataset. The original label distribution is non-uniform. See Appendix L for details.

## C TABLE OF NOTATION

## D PROOF OF THEOREM 1

In order to prove Theorem 1, we need to prove the expected transfer risk bound (i.e. Lemma 2).

**Lemma 2.** *If the prediction loss is assumed as $L$-Lipschitz and the hypothesis is $K$-Lipschitz w.r.t. the feature $x$ (given the same label), i.e. for $\forall Y = y$, $\|h(x_1, y) - h(x_2, y)\|_2 \leq K\|x_1 - x_2\|_2$. Then*

Table 8: Table of Notations

| | |
|---|---|
| $R_{\mathcal{D}}(h) = \mathbb{E}_{(x,y)\sim\mathcal{D}}\ell(h(x,y))$ | Expected Risk on distribution $\mathcal{D}$ w.r.t. hypothesis $h$ |
| $\hat{R}_{\mathcal{D}}(h) = \frac{1}{N}\sum_{i=1}^{N}\ell(h(x_i,y_i))$ | Empirical Risk on observed data $\{(x_i,y_i)\}_{i=1}^{N}$ that are i.i.d. sampled from $\mathcal{D}$. |
| $\alpha$ and $\hat{\alpha}_t$ | True and empirical label distribution ratio $\alpha(y) = \mathcal{T}(y)/\mathcal{S}(y)$ |
| $\hat{R}^{\alpha}_{\mathcal{S}}(h) = \frac{1}{N}\sum_{i=1}^{N}\alpha(y_i)\ell(h(x_i,y_i))$ | Empirical Weighted Risk on observed data $\{(x_i,y_i)\}_{i=1}^{N}$. |
| $\mathcal{S}(z\|y) = \int_x g(z\|x)S(x\|Y=y)dx$ | Conditional distribution w.r.t. latent variable $Z$ that induced by feature learning function $g$. |
| $W_1(\mathcal{S}_t(z\|y)\|\mathcal{T}(z\|y))$ | Conditional Wasserstein distance on the latent space $Z$ |

*the target risk can be upper bounded by:*

$$R_{\mathcal{T}}(h) \leq \sum_t \boldsymbol{\lambda}[t]R^{\alpha_t}_{\mathcal{S}}(h) + LK\sum_t \boldsymbol{\lambda}[t]\mathbb{E}_{y\sim\mathcal{T}(y)}W_1(\mathcal{T}(x|Y=y)\|\mathcal{S}(x|Y=y)) \tag{4}$$

*Proof.* The target risk can be expressed as:

$$R_{\mathcal{T}}(h(x,y)) = \mathbb{E}_{(x,y)\sim\mathcal{T}}\ell(h(x,y)) = \mathbb{E}_{y\sim\mathcal{T}(y)}\mathbb{E}_{x\sim\mathcal{T}(x|y)}\ell(h(x,y))$$

By denoting $\alpha(y) = \frac{\mathcal{T}(y)}{\mathcal{S}(y)}$, then we have:

$$\mathbb{E}_{y\sim\mathcal{T}(y)}\mathbb{E}_{y\sim\mathcal{T}(x|y)}\ell(h(x,y)) = \mathbb{E}_{y\sim\mathcal{S}(y)}\alpha(y)\mathbb{E}_{x\sim\mathcal{T}(x|y)}\ell(h(x,y))$$

Then we aim to upper bound $\mathbb{E}_{x\sim\mathcal{T}(x|y)}\ell(h(x,y))$. For any fixed $y$,

$$\mathbb{E}_{x\sim\mathcal{T}(x|y)}\ell(h(x,y)) - \mathbb{E}_{x\sim\mathcal{S}(x|y)}\ell(h(x,y)) \leq |\int_{x\in\mathcal{X}}\ell(h(x,y))d(\mathcal{T}(x|y) - \mathcal{S}(x|y))|$$

Then according to the Kantorovich-Rubinstein duality, for **any** distribution coupling $\gamma \in \Pi(\mathcal{T}(x|y), \mathcal{S}(x|y))$, then we have:

$$\begin{aligned}
&= \inf_{\gamma}|\int_{\mathcal{X}\times\mathcal{X}}\ell(h(x_p,y)) - \ell(h(x_q,y))d\gamma(x_p,x_q)| \\
&\leq \inf_{\gamma}\int_{\mathcal{X}\times\mathcal{X}}|\ell(h(x_p,y)) - \ell(h(x_q,y))|d\gamma(x_p,x_q) \\
&\leq L\inf_{\gamma}\int_{\mathcal{X}\times\mathcal{X}}|h(x_p,y)) - h(x_q,y)|d\gamma(x_p,x_q) \\
&\leq LK\inf_{\gamma}\int_{\mathcal{X}\times\mathcal{X}}\|x_p - x_q\|_2 d\gamma(x_p,x_q) \\
&= LKW_1(\mathcal{T}(x|Y=y)\|\mathcal{S}(x|Y=y))
\end{aligned}$$

The first inequality is obvious; and the second inequality comes from the assumption that $\ell$ is $L$-Lipschitz; the third inequality comes from the hypothesis is $K$-Lipschitz w.r.t. the feature $x$ (given the same label), i.e. for $\forall Y = y$, $\|h(x_1,y) - h(x_2,y)\|_2 \leq K\|x_1 - x_2\|_2$.

Then we have:

$$\begin{aligned}
R_{\mathcal{T}}(h) &\leq \mathbb{E}_{y\sim\mathcal{S}(y)}\alpha(y)[\mathbb{E}_{x\sim\mathcal{S}(x|y)}\ell(h(x,y)) + LKW_1(\mathcal{T}(x|y)\|\mathcal{S}(x|y))] \\
&= \mathbb{E}_{(x,y)\sim\mathcal{S}}\alpha(y)\ell(h(x,y)) + LK\mathbb{E}_{y\sim\mathcal{T}(y)}W_1(\mathcal{T}(x|Y=y)\|\mathcal{S}(x|Y=y)) \\
&= R^{\alpha}_{\mathcal{S}}(h) + LK\mathbb{E}_{y\sim\mathcal{T}(y)}W_1(\mathcal{T}(x|Y=y)\|\mathcal{S}(x|Y=y))
\end{aligned}$$

Supposing each source $\mathcal{S}_t$ we assign the weight $\boldsymbol{\lambda}[t]$ and label distribution ratio $\alpha_t(y) = \frac{\mathcal{T}(y)}{\mathcal{S}_t(y)}$, then by combining this $T$ source target pair, we have:

$$R_{\mathcal{T}}(h) \leq \sum_t \boldsymbol{\lambda}[t]R^{\alpha_t}_{\mathcal{S}_t}(h) + LK\sum_t \boldsymbol{\lambda}[t]\mathbb{E}_{y\sim\mathcal{T}(y)}W_1(\mathcal{T}(x|Y=y)\|\mathcal{S}_t(x|Y=y))$$

□

Then we will prove Theorem 1 from this result, we will derive the non-asymptotic bound, estimated from the finite sample observations. Supposing the empirical label ratio value is $\hat{\alpha}_t$, then for any simplex $\boldsymbol{\lambda}$ we can prove the high-probability bound.

### D.1 Bounding the empirical and expected prediction risk

*Proof.* We first bound the first term, which can be upper bounded as:

$$\sup_h |\sum_t \boldsymbol{\lambda}[t] R^{\alpha_t}_{\mathcal{S}_t}(h) - \sum_t \boldsymbol{\lambda}[t] \hat{R}^{\hat{\alpha}_t}_{\hat{\mathcal{S}}_t}(h)| \leq \underbrace{\sup_h |\sum_t \boldsymbol{\lambda}[t] R^{\alpha_t}_{\mathcal{S}_t}(h) - \sum_t \boldsymbol{\lambda}[t] \hat{R}^{\alpha_t}_{\hat{\mathcal{S}}_t}(h)|}_{\text{(I)}} + \underbrace{\sup_h |\sum_t \boldsymbol{\lambda}[t] \hat{R}^{\alpha_t}_{\hat{\mathcal{S}}_t}(h) - \sum_t \boldsymbol{\lambda}[t] \hat{R}^{\hat{\alpha}_t}_{\hat{\mathcal{S}}_t}(h)|}_{\text{(II)}}$$

**Bounding term (I)** According to the McDiarmid inequality, each item changes at most $|\frac{2\boldsymbol{\lambda}[t]\alpha_t(y)\ell}{N_{\mathcal{S}_t}}|$. Then we have:

$$P\left((\mathrm{I}) - \mathbb{E}(\mathrm{I}) \geq t\right) \leq \exp\left(\frac{-2t^2}{\sum_{t=1}^{T} \frac{4}{\beta_t N} \boldsymbol{\lambda}^2[t] \alpha_t(y)^2 \ell^2}\right) = \delta$$

By substituting $\delta$, at high probability $1-\delta$ we have:

$$(\mathrm{I}) \leq \mathbb{E}(\mathrm{I}) + L_{\max} d^{\sup}_{\infty} \sqrt{\sum_{t=1}^{T} \frac{\boldsymbol{\lambda}[t]^2}{\beta_t}} \sqrt{\frac{\log(1/\delta)}{2N}}$$

Where $L_{\max} = \sup_{h \in \mathcal{H}} \ell(h)$ and $N = \sum_{t=1}^{T} N_{\mathcal{S}_t}$ the total source observations and $\beta_t = \frac{N_{\mathcal{S}_t}}{N}$ the frequency ratio of each source. And $d^{\sup}_{\infty} = \max_{t=1,\ldots,T} d_{\infty}(\mathcal{T}(y) \| \mathcal{S}(y)) = \max_{t=1,\ldots,T} \max_{y \in [1,\mathcal{Y}]} \alpha_t(y)$, the maximum true label shift value (constant).

Bounding $\mathbb{E}\sup(\mathrm{I})$, the expectation term can be upper bounded as the form of Rademacher Complexity:

$$\begin{aligned}
\mathbb{E}(\mathrm{I}) &\leq 2\mathbb{E}_{\sigma}\mathbb{E}_{\hat{\mathcal{S}}_1^T} \sup_h \sum_{t=1}^{T} \boldsymbol{\lambda}[t] \sum_{(x_t,y_t) \in \hat{\mathcal{S}}_t} \frac{1}{TN} \left(\alpha_t(y)\ell(h(x_t,y_t))\right) \\
&\leq 2\sum_t \boldsymbol{\lambda}[t] \mathbb{E}_{\sigma}\mathbb{E}_{\hat{\mathcal{S}}_1^T} \sup_h \sum_{(x_t,y_t) \in \hat{\mathcal{S}}_t} \frac{1}{TN} \left(\alpha_t(y)\ell(h(x_t,y_t))\right) \\
&\leq 2\sup_t \mathbb{E}_{\sigma}\mathbb{E}_{\hat{\mathcal{S}}_t} \sup_h \sum_{(x_t,y_t) \in \hat{\mathcal{S}}_t} \frac{1}{TN} \left[\alpha_t(y)\ell(h(x_t,y_t))\right] \\
&= \sup_t 2\mathcal{R}_t(\ell, \mathcal{H}) = 2\bar{R}(\ell, \mathcal{H})
\end{aligned}$$

Where $\bar{R}(\ell, \mathcal{H}) = \sup_t \mathcal{R}_t(\ell, \mathcal{H}) = \sup_t \sup_{h \sim \mathcal{H}} \mathbb{E}_{\hat{\mathcal{S}}_t, \sigma} \sum_{(x_t,y_t) \in \hat{\mathcal{S}}_t} \frac{1}{TN} \left[\alpha_t(y)\ell(h(x_t,y_t))\right]$, represents the Rademacher complexity w.r.t. the prediction loss $\ell$, hypothesis $h$ and *true* label distribution ratio $\alpha_t$.

Therefore with high probability $1-\delta$, we have:

$$\sup_h |\sum_t \boldsymbol{\lambda}[t] R^{\alpha_t}_{\mathcal{S}}(h) - \sum_t \boldsymbol{\lambda}[t] \hat{R}^{\alpha_t}_{\mathcal{S}}(h)| \leq \bar{\mathcal{R}}(\ell, h) + L_{\max} d^{\sup}_{\infty} \sqrt{\sum_{t=1}^{T} \frac{\boldsymbol{\lambda}[t]^2}{\beta_t}} \sqrt{\frac{\log(1/\delta)}{2N}}$$

**Bounding Term (II)** For all the hypothesis $h$, we have:

$$\begin{aligned}
|\sum_t \boldsymbol{\lambda}[t] \hat{R}^{\alpha_t}_{\mathcal{S}_t}(h) - \sum_t \boldsymbol{\lambda}[t] \hat{R}^{\hat{\alpha}_t}_{\mathcal{S}_t}(h)| &= |\sum_t \boldsymbol{\lambda}[t] \frac{1}{N_{\mathcal{S}_t}} \sum_i^{N_{\mathcal{S}_t}} (\alpha(y(i)) - \hat{\alpha}(y(i)))\ell(h)| \\
&= \sum_t \boldsymbol{\lambda}[t] \frac{1}{N_{\mathcal{S}_t}} |\sum_y^{|\mathcal{Y}|} (\alpha(Y=y) - \hat{\alpha}(Y=y))\bar{\ell}(Y=y)|
\end{aligned}$$

Where $\bar{\ell}(Y=y)=\sum_i^{N_{\mathcal{S}_t}}\ell(h(x_i,y_i=y))$, represents the cumulative error, conditioned on a given label $Y=y$. According to the Holder inequality, we have:

$$\begin{aligned}\sum_t \boldsymbol{\lambda}[t]\frac{1}{N_{\mathcal{S}_t}}|\sum_y^{|\mathcal{Y}|}(\alpha_t(Y=y)-\hat{\alpha}_t(Y=y))\bar{\ell}(Y=y)| &\leq \sum_t \boldsymbol{\lambda}[t]\frac{1}{N_{\mathcal{S}_t}}\|\alpha_t-\hat{\alpha}_t\|_2\|\bar{\ell}(Y=y)\|_2\\ &\leq L_{\max}\sum_t \boldsymbol{\lambda}[t]\|\alpha_t-\hat{\alpha}_t\|_2\\ &\leq L_{\max}\sup_t\|\alpha_t-\hat{\alpha}_t\|_2\end{aligned}$$

Therefore, $\forall h\in\mathcal{H}$, with high probability $1-\delta$ we have:

$$\sum_t \boldsymbol{\lambda}[t]R_{\mathcal{S}}^{\alpha_t}(h)\leq\sum_t \boldsymbol{\lambda}[t]\hat{R}_{\mathcal{S}}^{\hat{\alpha}_t}(h)+2\bar{\mathcal{R}}(\ell,h)+L_{\max}d_{\infty}^{\sup}\sqrt{\sum_{t=1}^{T}\frac{\boldsymbol{\lambda}[t]^2}{\beta_t}}\sqrt{\frac{\log(1/\delta)}{2N}}+L_{\max}\sup_t\|\alpha_t-\hat{\alpha}_t\|_2$$

### D.2 Bounding empirical Wasserstein Distance

Then we need to derive the sample complexity of the empirical and true distributions, which can be decomposed as the following two parts. For any $t$, we have:

$$\begin{aligned}&\mathbb{E}_{y\sim\mathcal{T}(y)}W_1(\mathcal{T}(x|Y=y)\|\mathcal{S}_t(x|Y=y))-\mathbb{E}_{y\sim\hat{\mathcal{T}}(y)}W_1(\hat{\mathcal{T}}(x|Y=y)\|\hat{\mathcal{S}}_t(x|Y=y))\\ &\underbrace{\leq\mathbb{E}_{y\sim\mathcal{T}(y)}W_1(\mathcal{T}(x|Y=y)\|\mathcal{S}_t(x|Y=y))-\mathbb{E}_{y\sim\mathcal{T}(y)}W_1(\hat{\mathcal{T}}(x|Y=y)\|\hat{\mathcal{S}}_t(x|Y=y))}_{\text{(I)}}\\ &+\underbrace{\mathbb{E}_{y\sim\mathcal{T}(y)}W_1(\hat{\mathcal{T}}(x|Y=y)\|\hat{\mathcal{S}}_t(x|Y=y))-\mathbb{E}_{y\sim\hat{\mathcal{T}}(y)}W_1(\hat{\mathcal{T}}(x|Y=y)\|\hat{\mathcal{S}}_t(x|Y=y))}_{\text{(II)}}\end{aligned}$$

**Bounding (I)** We have:

$$\begin{aligned}&\mathbb{E}_{y\sim\mathcal{T}(y)}W_1(\mathcal{T}(x|Y=y)\|\mathcal{S}_t(x|Y=y))-\mathbb{E}_{y\sim\mathcal{T}(y)}W_1(\hat{\mathcal{T}}(x|Y=y)\|\hat{\mathcal{S}}_t(x|Y=y))\\ &=\sum_y\mathcal{T}(y)\Big(W_1(\mathcal{T}(x|Y=y)\|\mathcal{S}_t(x|Y=y))-W_1(\hat{\mathcal{T}}(x|Y=y)\|\hat{\mathcal{S}}_t(x|Y=y)\Big)\\ &\leq|\sum_y\mathcal{T}(y)|\sup_y\Big(W_1(\mathcal{T}(x|Y=y)\|\mathcal{S}_t(x|Y=y))-W_1(\hat{\mathcal{T}}(x|Y=y)\|\hat{\mathcal{S}}_t(x|Y=y)\Big)\\ &=\sup_y\Big(W_1(\mathcal{T}(x|Y=y)\|\mathcal{S}_t(x|Y=y))-W_1(\hat{\mathcal{T}}(x|Y=y)\|\hat{\mathcal{S}}_t(x|Y=y)\Big)\\ &\leq\sup_y\ [W_1(\mathcal{S}_t(x|Y=y)\|\hat{\mathcal{S}}_t(x|Y=y))+W_1(\hat{\mathcal{S}}_t(x|Y=y)\|\hat{\mathcal{T}}(x|Y=y))\\ &+W_1(\hat{\mathcal{T}}(x|Y=y)\|\mathcal{T}(x|Y=y))-W_1(\hat{\mathcal{T}}(x|Y=y)\|\hat{\mathcal{S}}_t(x|Y=y))]\\ &=\sup_y W_1(\mathcal{S}_t(x|Y=y)\|\hat{\mathcal{S}}_t(x|Y=y))+W_1(\hat{\mathcal{T}}(x|Y=y)\|\mathcal{T}(x|Y=y))\end{aligned}$$

The first inequality holds because of the Holder inequality. As for the second inequality, we use the triangle inequality of Wasserstein distance. $W_1(P\|Q)\leq W_1(P\|P_1)+W_1(P_1\|P_2)+W_1(P_2\|Q)$.

According to the convergence behavior of Wasserstein distance (Weed et al., 2019), with high probability $\geq 1-2\delta$ we have:

$$W_1(\mathcal{S}_t(x|Y=y)\|\hat{\mathcal{S}}_t(x|Y=y))+W_1(\hat{\mathcal{T}}(x|Y=y)\|\mathcal{T}(x|Y=y))\leq\kappa(\delta,N_{\mathcal{S}_t}^y,N_{\mathcal{T}}^y)$$

Where $k(\delta,N_{\mathcal{S}_t}^y,N_{\mathcal{T}}^y)=C_{t,y}(N_{\mathcal{S}_t}^y)^{-s_{t,y}}+C_y(N_{\mathcal{T}}^y)^{-s_y}+\sqrt{\frac{1}{2}\log(\frac{2}{\delta})}(\sqrt{\frac{1}{N_{\mathcal{S}_t}^y}}+\sqrt{\frac{1}{N_t^y}})$, where $N_{\mathcal{S}_t}^y$ is the number of $Y=y$ in source $t$ and $N_{\mathcal{T}}^y$ is the number of $Y=y$ in target distribution. $C_{t,y}$, $C_y$ $s_{t,y}>2$, $s_y>2$ are positive constant in the concentration inequality. This indicates the convergence behavior between empirical and true Wasserstein distance.

If we adopt the union bound (over all the labels) by setting $\delta \leftarrow \delta/|\mathcal{Y}|$, then with high probability $\geq 1-2\delta$, we have:

$$\sup_y W_1(\mathcal{S}(x|Y=y)\|\hat{\mathcal{S}}(x|Y=y)) + W_1(\hat{\mathcal{T}}(x|Y=y)\|\mathcal{T}(x|Y=y)) \leq \kappa(\delta, N^y_{\mathcal{S}_t}, N^y_{\mathcal{T}})$$

where $\kappa(\delta, N^y_{\mathcal{S}_t}, N^y_{\mathcal{T}}) = C_{t,y}(N^y_{\mathcal{S}_t})^{-s_{t,y}} + C_y(N^y_{\mathcal{T}})^{-s_y} + \sqrt{\frac{1}{2}\log(\frac{2|\mathcal{Y}|}{\delta})}(\sqrt{\frac{1}{N^y_{\mathcal{S}_t}}} + \sqrt{\frac{1}{N^y_{\mathcal{T}}}})$

Again by adopting the union bound (over all the tasks) by setting $\delta \leftarrow \delta/T$, with high probability $\geq 1-2\delta$, we have:

$$\sum_t \boldsymbol{\lambda}[t]\mathbb{E}_{y\sim\mathcal{T}(y)}W_1(\mathcal{T}(x|Y=y)\|\mathcal{S}(x|Y=y)) - \sum_t \boldsymbol{\lambda}[t]\mathbb{E}_{y\sim\mathcal{T}(y)}W_1(\hat{\mathcal{T}}(x|Y=y)\|\hat{\mathcal{S}}(x|Y=y)) \leq \sup_t \kappa(\delta, N^y_{\mathcal{S}_t}, N^y_{\mathcal{T}})$$

Where $\kappa(\delta, N^y_{\mathcal{S}_t}, N^y_{\mathcal{T}}) = C_{t,y}(N^y_{\mathcal{S}_t})^{-s_{t,y}} + C_y(N^y_{\mathcal{T}})^{-s_y} + \sqrt{\frac{1}{2}\log(\frac{2T|\mathcal{Y}|}{\delta})}(\sqrt{\frac{1}{N^y_{\mathcal{S}_t}}} + \sqrt{\frac{1}{N^y_{\mathcal{T}}}})$.

**Bounding (II)** We can bound the second term:

$$\begin{aligned}
&\mathbb{E}_{y\sim\mathcal{T}(y)}W_1(\hat{\mathcal{T}}(x|Y=y)\|\hat{\mathcal{S}}_t(x|Y=y)) - \mathbb{E}_{y\sim\hat{\mathcal{T}}(y)}W_1(\hat{\mathcal{T}}(x|Y=y)\|\hat{\mathcal{S}}_t(x|Y=y)) \\
&\leq \sup_y W_1(\hat{\mathcal{T}}(x|Y=y)\|\hat{\mathcal{S}}_t(x|Y=y))|\sum_y \mathcal{T}(y) - \hat{\mathcal{T}}(y)| \\
&\leq C^t_{\text{max}}|\sum_y \mathcal{T}(y) - \hat{\mathcal{T}}(y)|
\end{aligned}$$

Where $C^t_{\text{max}} = \sup_y W_1(\hat{\mathcal{T}}(x|Y=y)\|\hat{\mathcal{S}}(x|Y=y))$ is a positive and bounded constant. Then we need to bound $|\sum_y \mathcal{T}(y) - \hat{\mathcal{T}}(y)|$, by adopting MicDiarmid's inequality, we have at high probability $1-\delta$:

$$\begin{aligned}
|\sum_y \mathcal{T}(y) - \hat{\mathcal{T}}(y)| &\leq \mathbb{E}_{\hat{\mathcal{T}}}|\sum_y \mathcal{T}(y) - \hat{\mathcal{T}}(y)| + \sqrt{\frac{\log(1/\delta)}{2N_{\mathcal{T}}}} \\
&= 2\mathbb{E}_\sigma\mathbb{E}_{\hat{\mathcal{T}}}\sum_y \sigma\hat{\mathcal{T}}(y) + \sqrt{\frac{\log(1/\delta)}{2N_{\mathcal{T}}}}
\end{aligned}$$

Then we bound $\mathbb{E}_\sigma\mathbb{E}_{\hat{\mathcal{T}}}\sum_y \sigma\hat{\mathcal{T}}(y)$. We use the properties of Rademacher complexity [Lemma 26.11, (Shalev-Shwartz & Ben-David, 2014)] and notice that $\hat{\mathcal{T}}(y)$ is a probability simplex, then we have:

$$\mathbb{E}_\sigma\mathbb{E}_{\hat{\mathcal{T}}}\sum_y \sigma\hat{\mathcal{T}}(y) \leq \sqrt{\frac{2\log(2|\mathcal{Y}|)}{N_{\mathcal{T}}}}$$

Then we have $|\sum_y \mathcal{T}(y) - \hat{\mathcal{T}}(y)| \leq \sqrt{\frac{2\log(2|\mathcal{Y}|)}{N_{\mathcal{T}}}} + \sqrt{\frac{\log(1/\delta)}{2N_{\mathcal{T}}}}$

Then using the union bound and denoting $\delta \leftarrow \delta/T$, with high probability $\geq 1-\delta$ and for any simplex $\boldsymbol{\lambda}$, we have:

$$\sum_t \boldsymbol{\lambda}[t]\mathbb{E}_{y\sim\mathcal{T}(y)}W_1(\hat{\mathcal{T}}(x|Y=y)\|\hat{\mathcal{S}}_t(x|Y=y)) \leq \sum_t \boldsymbol{\lambda}[t]\mathbb{E}_{y\sim\hat{\mathcal{T}}(y)}W_1(\hat{\mathcal{T}}(x|Y=y)\|\hat{\mathcal{S}}_t(x|Y=y))$$
$$C_{\max}(\sqrt{\frac{2\log(2|\mathcal{Y}|)}{N_{\mathcal{T}}}} + \sqrt{\frac{\log(T/\delta)}{2N_{\mathcal{T}}}})$$

where $C_{\max} = \sup_t C^t_{\max}$.

Combining together, we can derive the PAC-Learning bound, which is estimated from the finite samples (with high probability $1-4\delta$):

$$\begin{aligned}
R_{\mathcal{T}}(h) \leq &\sum_t \boldsymbol{\lambda}_t \hat{R}^{\hat{\alpha}_t}_{\mathcal{S}_t}(h) + LH\sum_t \boldsymbol{\lambda}_t\mathbb{E}_{y\sim\hat{\mathcal{T}}(y)}W_1(\hat{\mathcal{T}}(x|Y=y)\|\hat{\mathcal{S}}(x|Y=y)) + L_{\max}d^{\sup}_\infty\sqrt{\sum_{t=1}^T \frac{\boldsymbol{\lambda}_t^2}{\beta_t}}\sqrt{\frac{\log(1/\delta)}{2N}} \\
&+ 2\bar{\mathcal{R}}(\ell, h) + L_{\max}\sup_t\|\alpha_t - \hat{\alpha}_t\|_2 + \sup_t \kappa(\delta, N^y_{\mathcal{S}_t}, N^y_{\mathcal{T}}) + C_{\max}(\sqrt{\frac{2\log(2|\mathcal{Y}|)}{N_{\mathcal{T}}}} + \sqrt{\frac{\log(T/\delta)}{2N_{\mathcal{T}}}})
\end{aligned}$$

Then we denote $\text{Comp}(N_{\mathcal{S}_1}, \ldots, N_{\mathcal{T}}, \delta) = 2\bar{\mathcal{R}}(\ell, h) + \sup_t \kappa(\delta, N^y_{\mathcal{S}_t}, N^y_{\mathcal{T}}) + C_{\max}(\sqrt{\frac{2\log(2|\mathcal{Y}|)}{N_{\mathcal{T}}}} + \sqrt{\frac{\log(T/\delta)}{2N_{\mathcal{T}}}})$ as the convergence rate function that decreases with larger $N_{\mathcal{S}_1}, \ldots, N_{\mathcal{T}}$. Bedsides, $\bar{\mathcal{R}}(\ell, h) = \sup_t \mathcal{R}_t(\ell, \mathcal{H})$ is the re-weighted Rademacher complexity. Given a fixed hypothesis with finite VC dimension [3], it can be proved $\bar{\mathcal{R}}(\ell, h) = \min_{N_{\mathcal{S}_1}, \ldots, N_{\mathcal{S}_T}} \mathcal{O}(\sqrt{\frac{1}{N_{\mathcal{S}_t}}})$ i.e (Shalev-Shwartz & Ben-David, 2014). □

## E PROOF OF THEOREM 2

We first recall the stochastic feature representation $g$ such that $g : \mathcal{X} \to \mathcal{Z}$ and *scoring hypothesis* h $h : \mathcal{Z} \times \mathcal{Y} \to \mathbb{R}$ and the prediction loss $\ell$ with $\ell : \mathbb{R} \to \mathbb{R}$. [4]

*Proof.* The marginal distribution and conditional distribution w.r.t. latent variable $Z$ that are induced by $g$, which can be reformulated as:

$$\mathcal{S}(z) = \int_x g(z|x)\mathcal{S}(x)dx \qquad \mathcal{S}(z|y) = \int_x g(z|x)\mathcal{S}(x|Y = y)dx$$

In the multi-class classification problem, we additionally define the following distributions:

$$\mu^k(z) = \mathcal{S}(Y = k, z) = \mathcal{S}(Y = k)\mathcal{S}(z|Y = k)$$
$$\pi^k(z) = \mathcal{T}(Y = k, z) = \mathcal{T}(Y = k)\mathcal{T}(z|Y = k)$$

Based on (Nguyen et al., 2009) and $g(z|x)$ is a stochastic representation learning function, the loss conditioned a fixed point $(x, y)$ w.r.t. $h$ and $g$ is $\mathbb{E}_{z\sim g(z|x)}\ell(h(z, y))$. Then taking the expectation over the $\mathcal{S}(x, y)$ we have: [5]

$$\begin{aligned}
R_{\mathcal{S}}(h, g) &= \mathbb{E}_{(x,y)\sim\mathcal{S}(x,y)}\mathbb{E}_{z\sim g(z|x)}\ell(h(z, y)) \\
&= \sum_{k=1}^{|\mathcal{Y}|} \mathcal{S}(y = k) \int_x \mathcal{S}(x|Y = k) \int_z g(z|x)\ell(h(z, y = k))dzdx \\
&= \sum_{k=1}^{|\mathcal{Y}|} \mathcal{S}(y = k) \int_z [\int_x \mathcal{S}(x|Y = k)g(z|x)dx]\ell(h(z, y = k))dz \\
&= \sum_{k=1}^{|\mathcal{Y}|} \mathcal{S}(y = k) \int_z \mathcal{S}(z|Y = k)\ell(h(z, y = k))dz \\
&= \sum_{k=1}^{|\mathcal{Y}|} \int_z \mathcal{S}(z, Y = k)\ell(h(z, y = k))dz \\
&= \sum_{k=1}^{|\mathcal{Y}|} \int_z \mu^k(z)\ell(h(z, y = k))dz
\end{aligned}$$

[3] If the hypothesis is the neural network, the Rademacher complexity can still be bounded analogously.

[4] Note this definition is different from the conventional binary classification with binary output, and it is more suitable in the multi-classification scenario and cross entropy loss (Hoffman et al., 2018a). For example, if we define $l = -\log(\cdot)$ and $h(z, y) \in (0, 1)$ as a scalar score output. Then $\ell(h(z, y))$ can be viewed as the cross-entropy loss for the neural-network.

[5] An alternative understanding is based on the Markov chain. In this case it is a DAG with $Y \xleftarrow{\mathcal{S}(y|x)} X \xrightarrow{g} Z$, $X \xrightarrow{\mathcal{S}(y|x)} Y \xrightarrow{h} S \xleftarrow{h} Z \xleftarrow{g} X$. (S is the output of the scoring function). Then the expected loss over the all random variable can be equivalently written as $\int \mathbb{P}(x, y, z, s)\ \ell(s)\ d(x, y, z, s) = \int \mathbb{P}(x)\mathbb{P}(y|x)\mathbb{P}(z|x)\mathbb{P}(s|z, y)\ell(s) = \int \mathbb{P}(x, y)\mathbb{P}(z|x)\mathbb{P}(s|z, y)\ell(s)d(x, y)d(z)d(s)$. Since the scoring $S$ is determined by $h(x, y)$, then $\mathbb{P}(s|y, z) = 1$. According to the definition we have $\mathbb{P}(z|x) = g(z|x)$, $\mathbb{P}(x, y) = \mathcal{S}(x, y)$, then the loss can be finally expressed as $\mathbb{E}_{\mathcal{S}(x,y)}\mathbb{E}_{g(z|x)}\ell(h(z, y))$

Intuitively, the expected loss w.r.t. the joint distribution $\mathcal{S}$ can be decomposed as the expected loss on the label distribution $\mathcal{S}(y)$ (weighted by the labels) and conditional distribution $\mathcal{S}(\cdot|y)$ (real valued conditional loss).

Then the expected risk on the $\mathcal{S}$ and $\mathcal{T}$ can be expressed as:

$$R_{\mathcal{S}}(h,g) = \sum_{k=1}^{|\mathcal{Y}|} \int_z \ell(h(z, y=k))\mu^k(z)dz$$

$$R_{\mathcal{T}}(h,g) = \sum_{k=1}^{|\mathcal{Y}|} \int_z \ell(h(z, y=k))\pi^k(z)dz$$

By denoting $\alpha(y) = \frac{\mathcal{T}(y)}{\mathcal{S}(y)}$, we have the $\alpha$-weighted loss:

$$\begin{aligned} R^{\alpha}_{\mathcal{S}}(h,g) =& \mathcal{T}(Y=1)\int_z \ell(h(z,y=1))\mathcal{S}(z|Y=1) + \mathcal{T}(Y=2)\int_z \ell(h(z,y=2))\mathcal{S}(z|Y=2) \\ &+ \cdots + \mathcal{T}(Y=k)\int_z \ell(h(z,y=k))\mathcal{S}(z|Y=k)dz \end{aligned}$$

Then we have:

$$R_{\mathcal{T}}(h,g) - R^{\alpha}_{\mathcal{S}}(h,g) \leq \sum_k \mathcal{T}(Y=k)\int_z \ell(h(z,y=k))d|\mathcal{S}(z|Y=k) - \mathcal{T}(z|Y=k)|$$

Under the same assumption, we have the loss function $\ell(h(z, Y=k))$ is KL-Lipschitz w.r.t. the cost $\|\cdot\|_2$ (given a fixed $k$). Therefore by adopting the same proof strategy (Kantorovich-Rubinstein duality) in Lemma 2, we have

$$\begin{aligned} &\leq KL\mathcal{T}(Y=1)W_1(\mathcal{S}(z|Y=1)\|\mathcal{T}(z|Y=1)) + \cdots + KL\mathcal{T}(Y=k)W_1(\mathcal{S}(z|Y=k)\|\mathcal{T}(z|Y=k)) \\ &= KL\mathbb{E}_{y\sim\mathcal{T}(y)}W_1(\mathcal{S}(z|Y=y)\|\mathcal{T}(z|Y=y)) \end{aligned}$$

Therefore, we have:

$$R_{\mathcal{T}}(h,g) \leq R^{\alpha}_{\mathcal{S}}(h,g) + LK\mathbb{E}_{y\sim\mathcal{T}(y)}W_1(\mathcal{S}(z|Y=y)\|\mathcal{T}(z|Y=y))$$

Based on the aforementioned result, we have $\forall t = 1, \ldots, T$ and denote $\mathcal{S} = \mathcal{S}_t$ and $\alpha(y) = \alpha_t(y) = \mathcal{T}(y)/\mathcal{S}_t(y)$:

$$\boldsymbol{\lambda}[t]R_{\mathcal{T}}(h,g) \leq \boldsymbol{\lambda}[t]R^{\alpha_t}_{\mathcal{S}_t}(h,g) + LK\boldsymbol{\lambda}[t]\mathbb{E}_{y\sim\mathcal{T}(y)}W_1(\mathcal{S}_t(z|Y=y)\|\mathcal{T}(z|Y=y))$$

Summing over $t = 1, \ldots, T$, we have:

$$R_{\mathcal{T}}(h,g) \leq \sum_{t=1}^{T}\boldsymbol{\lambda}[t]R^{\alpha_t}_{\mathcal{S}_t}(h,g) + LK\sum_{t=1}^{T}\boldsymbol{\lambda}[t]\mathbb{E}_{y\sim\mathcal{T}(y)}W_1(\mathcal{S}_t(z|Y=y)\|\mathcal{T}(z|Y=y))$$

□

## F APPROXIMATION $W_1$ DISTANCE

According to Jensen inequality, we have

$$W_1(\hat{\mathcal{S}}_t(z|Y=y)\|\hat{\mathcal{T}}(z|Y=y)) \leq \sqrt{[W_2(\hat{\mathcal{S}}_t(z|Y=y)\|\hat{\mathcal{T}}(z|Y=y))]^2}$$

Supposing $\hat{\mathcal{S}}_t(z|Y=y) \approx \mathcal{N}(\mathbf{C}^y_t, \boldsymbol{\Sigma})$ and $\hat{\mathcal{T}}(z|Y=y) \approx \mathcal{N}(\mathbf{C}^y, \boldsymbol{\Sigma})$, then we have:

$$[W_2(\hat{\mathcal{S}}_t(z|Y=y)\|\hat{\mathcal{T}}(z|Y=y)]^2 = \|\mathbf{C}^y_t - \mathbf{C}^y\|^2_2 + \text{Trace}(2\boldsymbol{\Sigma} - 2(\boldsymbol{\Sigma}\boldsymbol{\Sigma})^{1/2}) = \|\mathbf{C}^y_t - \mathbf{C}^y\|^2_2$$

We would like to point out that assuming the identical covariance matrix is more computationally efficient during the matching. This is advantageous and reasonable in the deep learning regime: we adopted the mini-batch (ranging from 20-128) for the neural network parameter optimization, in each mini-batch the samples of each class are **small**, then we compute the empirical covariance/variance matrix will be surely **biased** to the ground truth variance and induce a much higher complexity to optimize. By the contrary, the empirical mean is **unbiased** and computationally efficient, we can simply use the moving the moving average to efficiently update the estimated mean value (with a unbiased estimator). The empirical results verify the effectiveness of this idea.

## G PROOF OF LEMMA 1

For each source $\mathcal{S}_t$, by introducing the duality of Wasserstein-1 distance, for $y \in \mathcal{Y}$, we have:

$$\begin{aligned} W_1(\mathcal{S}_t(z|y)\|\mathcal{T}(z|y)) &= \sup_{\|d\|_L \leq 1} \mathbb{E}_{z\sim\mathcal{S}_t(z|y)} d(z) - \mathbb{E}_{z\sim\mathcal{T}(z|y)} d(z) \\ &= \sup_{\|d\|_L \leq 1} \sum_z \mathcal{S}_t(z|y) d(z) - \sum_z \mathcal{T}(z|y) d(z) \\ &= \frac{1}{\mathcal{T}(y)} \sup_{\|d\|_L \leq 1} \frac{\mathcal{T}(y)}{\mathcal{S}_t(y)} \sum_z \mathcal{S}_t(z,y) d(z) - \sum_z \mathcal{T}(z,y) d(z) \end{aligned}$$

Then by defining $\bar{\alpha}_t(z) = \mathbf{1}_{\{(z,y)\sim\mathcal{S}_t\}} \frac{\mathcal{T}(Y=y)}{\mathcal{S}_t(Y=y)} = \mathbf{1}_{\{(z,y)\sim\mathcal{S}_t\}} \alpha_t(Y=y)$, we can see for each pair observation $(z, y)$ sampled from the same distribution, then $\bar{\alpha}_t(Z = z) = \alpha_t(Y = y)$. Then we have:

$$\begin{aligned} \sum_y \mathcal{T}(y) W_1(\mathcal{S}_t(z|y)\|\mathcal{T}(z|y)) &= \sum_y \sup_{\|d\|_L \leq 1} \{\sum_z \alpha_t(y) \mathcal{S}_t(z,y) d(z) - \sum_z \mathcal{T}(z,y) d(z)\} \\ &= \sup_{\|d\|_L \leq 1} \sum_z \bar{\alpha}_t(z) \mathcal{S}_t(z) d(z) - \sum_z \mathcal{T}(z) d(z) \\ &= \sup_{\|d\|_L \leq 1} \mathbb{E}_{z\sim\mathcal{S}_t(z)} \bar{\alpha}_t(z) d(z) - \mathbb{E}_{z\sim\mathcal{T}(z)} d(z) \end{aligned}$$

We propose a simple example to understand $\bar{\alpha}_t$: supposing three samples in $\mathcal{S}_t = \{(z_1, Y = 1), (z_2, Y = 1), (z_3, Y = 0)\}$ then $\bar{\alpha}_t(z_1) = \bar{\alpha}_t(z_2) = \alpha_t(1)$ and $\bar{\alpha}_t(z_3) = \alpha_t(0)$. Therefore, the conditional term is equivalent to the label-weighted Wasserstein adversarial learning. We plug in each source domain as weight $\boldsymbol{\lambda}[t]$ and domain discriminator as $d_t$, we finally have Lemma 1.

## H DERIVE THE LABEL RATIO LOSS

We suppose the representation learning aims at matching the conditional distribution such that $\mathcal{T}(z|y) \approx \mathcal{S}_t(z|y)$,$\forall t$, then we suppose the predicted target distribution as $\bar{\mathcal{T}}(y)$. By simplifying the notation, we define $f(z) = \text{argmax}_y h(z, y)$ the most possible prediction label output, then we have:

$$\begin{aligned} \bar{\mathcal{T}}(y) &= \sum_{k=1}^{\mathcal{Y}} \mathcal{T}(f(z) = y|Y = k)\mathcal{T}(Y = k) = \sum_{k=1}^{\mathcal{Y}} \mathcal{S}_t(f(z) = y|Y = k)\mathcal{T}(Y = k) \\ &= \sum_{i=1}^{\mathcal{Y}} \mathcal{S}_t(f(z) = y, Y = k)\alpha_t(k) = \bar{\mathcal{T}}_{\alpha_t}(y) \end{aligned}$$

The first equality comes from the definition of target label prediction distribution, $\bar{\mathcal{T}}(y) = \mathbb{E}_{\mathcal{T}(z)} \mathbf{1}\{f(z) = y\} = \mathcal{T}(f(z) = y) = \sum_{k=1}^{\mathcal{Y}} \mathcal{T}(f(z) = y, Y = k) = \sum_{k=1}^{\mathcal{Y}} \mathcal{T}(f(z) = y|Y = k)\mathcal{T}(Y = k)$.

The second equality $\mathcal{T}(f(z) = y|Y = k) = \mathcal{S}_t(f(z) = y|Y = k)$ holds since $\forall t$, $\mathcal{T}(z|y) \approx \mathcal{S}_t(z|y)$, then for the shared hypothesis $f$, we have $\mathcal{T}(f(z) = y|Y = k) = \mathcal{S}_t(f(z) = y|Y = k)$.

The term $\mathcal{S}_t(f(z) = y, Y = k)$ is the (expected) source prediction confusion matrix, and we denote its empirical (observed) version as $\hat{\mathcal{S}}_t(f(z) = y, Y = k)$.

Based on this idea, in practice we want to find a $\hat{\alpha}_t$ to match the two predicted distribution $\bar{\mathcal{T}}$ and $\bar{\mathcal{T}}_{\hat{\alpha}_t}$. If we adopt the KL-divergence as the metric, we have:

$$\begin{aligned} \min_{\hat{\alpha}_t} D_{\text{KL}}(\bar{\mathcal{T}}\|\bar{\mathcal{T}}_{\hat{\alpha}_t}) &= \min_{\hat{\alpha}_t} \mathbb{E}_{y\sim\bar{\mathcal{T}}} \log(\frac{\bar{\mathcal{T}}(y)}{\bar{\mathcal{T}}_{\hat{\alpha}_t}(y)}) = \min_{\hat{\alpha}_t} -\mathbb{E}_{y\sim\bar{\mathcal{T}}} \log(\bar{\mathcal{T}}_{\hat{\alpha}_t}(y)) \\ &= \min_{\hat{\alpha}_t} -\sum_y \bar{\mathcal{T}}(y) \log(\sum_{k=1}^{\mathcal{Y}} \mathcal{S}_t(f(z) = y, Y = k)\hat{\alpha}_t(k)) \end{aligned}$$

We should notice the nature constraints of label ratio: $\{\hat{\alpha}_t(y) \geq 0, \sum_y \hat{\alpha}_t(y)\hat{\mathcal{S}}_t(y) = 1\}$. Based on this principle, we proposed the optimization problem to estimate each label ratio. We adopt its empirical counterpart, the empirical confusion matrix $C_{\hat{\mathcal{S}}_t}[y,k] = \hat{\mathcal{S}}_t[f(z) = y, Y = k]$, then the optimization loss can be expressed as:

$$\begin{aligned} \min_{\hat{\alpha}_t} \quad & -\sum_{y=1}^{|\mathcal{Y}|} \bar{\mathcal{T}}(y) \log(\sum_{k=1}^{|\mathcal{Y}|} C_{\hat{\mathcal{S}}_t}[y,k]\hat{\alpha}_t(k)) \\ \text{s.t.} \quad & \forall y \in \mathcal{Y}, \hat{\alpha}_t(y) \geq 0, \quad \sum_y \hat{\alpha}_t(y)\hat{\mathcal{S}}_t(y) = 1 \end{aligned}$$

# I LABEL PARTIAL MULTI-SOURCE UNSUPERVISED DA

The key difference between multi-conventional and partial unsupervised DA is the estimation step of $\hat{\alpha}_t$. In fact, we only add a sparse constraint for estimating each $\hat{\alpha}_t$:

$$\begin{aligned} \min_{\hat{\alpha}_t} \quad & -\sum_{y=1}^{|\mathcal{Y}|} \bar{\mathcal{T}}(y) \log(\sum_{k=1}^{|\mathcal{Y}|} C_{\hat{\mathcal{S}}_t}[y,k]\hat{\alpha}_t(k)) + C_2\|\hat{\alpha}_t\|_1 \\ \text{s.t.} \quad & \forall y \in \mathcal{Y}, \hat{\alpha}_t(y) \geq 0, \quad \sum_y \hat{\alpha}_t(y)\hat{\mathcal{S}}_t(y) = 1 \end{aligned} \tag{5}$$

Where $C_2$ is the hyper-parameter to control the level of target label sparsity, to estimate the target label distribution. In the paper, we denote $C_2 = 0.1$.

# J EXPLICIT AND IMPLICIT CONDITIONAL LEARNING

Inspired by Theorem 2, we need to learn the function $g : \mathcal{X} \to \mathcal{Z}$ and $h : \mathcal{Z} \times \mathcal{Y} \to \mathbb{R}$ to minimize:

$$\min_{g,h} \sum_t \boldsymbol{\lambda}[t]\hat{R}^{\hat{\alpha}_t}_{\mathcal{S}_t}(h,g) + C_0 \sum_t \boldsymbol{\lambda}[t]\mathbb{E}_{y\sim\hat{\mathcal{T}}(y)} W_1(\hat{\mathcal{S}}_t(z|Y=y)\|\hat{\mathcal{T}}(z|Y=y))$$

This can be equivalently expressed as:

$$\begin{aligned} \min_{g,h} \sum_t \boldsymbol{\lambda}[t]\hat{R}^{\alpha_t}_{\mathcal{S}_t}(h,g) &+ \epsilon C_0 \sum_t \boldsymbol{\lambda}[t]\mathbb{E}_{y\sim\hat{\mathcal{T}}(y)} W_1(\hat{\mathcal{S}}_t(z|Y=y)\|\hat{\mathcal{T}}(z|Y=y)) \\ &+ (1-\epsilon)C_0 \sum_t \boldsymbol{\lambda}[t]\mathbb{E}_{y\sim\hat{\mathcal{T}}(y)} W_1(\hat{\mathcal{S}}_t(z|Y=y)\|\hat{\mathcal{T}}(z|Y=y)) \end{aligned}$$

Due to the explicit and implicit approximation of conditional distance, we then optimize an alternative form:

$$\begin{aligned} \min_{g,h} \max_{d_1,\ldots,d_T} \underbrace{\sum_t \boldsymbol{\lambda}[t]\hat{R}^{\hat{\alpha}_t}_{\mathcal{S}_t}(h,g)}_{\text{Classification Loss}} &+ \epsilon C_0 \underbrace{\sum_t \boldsymbol{\lambda}[t]\mathbb{E}_{y\sim\hat{\mathcal{T}}(y)}\|\mathbf{C}^y_t - \mathbf{C}^y\|_2}_{\text{Explicit Conditional Loss}} \\ &+ (1-\epsilon)C_0 \underbrace{\sum_t \boldsymbol{\lambda}[t][\mathbb{E}_{z\sim\hat{\mathcal{S}}_t(z)}\bar{\alpha}^t(z)d(z) - \mathbb{E}_{z\sim\hat{\mathcal{T}}(z)}d(z)]}_{\text{Implicit Conditional Loss}} \end{aligned} \tag{6}$$

Where

- $\mathbf{C}^y_t = \sum_{(z_t,y_t)\sim\hat{\mathcal{S}}_t} \mathbf{1}_{\{y_t=y\}} z_t$ the centroid of label $Y = y$ in source $\mathcal{S}_t$.
- $\mathbf{C}^y = \sum_{(z_t,y_p)\sim\hat{\mathcal{T}}} \mathbf{1}_{\{y_p=y\}} z_t$ the centroid of pseudo-label $Y = y_p$ in target $\mathcal{S}_t$. (If it is the unsupervised DA scenarios).
- $\bar{\alpha}_t(z) = \mathbf{1}_{\{(z,y)\sim\mathcal{S}_t\}}\hat{\alpha}_t(Y = y)$, namely if each pair observation $(z, y)$ from the distribution, then $\bar{\alpha}_t(Z = z) = \hat{\alpha}_t(Y = y)$.

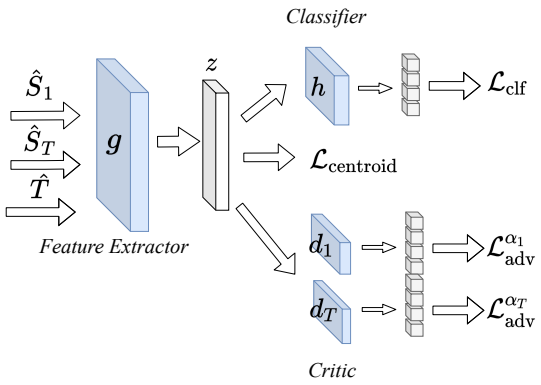


Figure 4: Network Structure of Proposed Approach. It consists three losses: the weighted Classification losses; the centroid matching for explicit conditional matching; the weighted adversarial loss for implicit conditional matching, showed in Eq. (6)

- $d_1, \cdots, d_T$ are domain discriminator (or critic function) restricted within 1-Lipschitz function.
- $\epsilon \in [0, 1]$ is the adjustment parameter in the trade-off of explicit and implicit learning. Based on the equivalence form, our approach proposed a theoretical principled way to tuning its weights. In the paper, we assume $\epsilon = 0.5$.
- $\hat{\mathcal{T}}(y)$ empirical target label distribution. (In the unsupervised DA scenarios, we approximate it by predicted target label distribution $\bar{\mathcal{T}}(y)$.)

**Gradient Penalty** In order to enforce the Lipschitz property of the statistic critic function, we adopt the gradient penalty term (Gulrajani et al., 2017). More concretely, given two samples $z_s \sim \mathcal{S}_t(z)$ and $z_t \sim \mathcal{T}(z)$ we generate an interpolated sample $z_{\text{int}} = \xi z_s + (1 - \xi) z_t$ with $\xi \sim \text{Unif}[0, 1]$. Then we add a gradient penalty $\|\nabla d(z_{\text{int}})\|_2^2$ as a regularization term to control the Lipschitz property w.r.t. the discriminator $d_1, \cdots, d_T$.

## K Algorithm Descriptions

We propose a detailed pipeline of the proposed algorithm in the following, shown in Algorithm 2 and 3. As for updating $\boldsymbol{\lambda}$ and $\alpha_t$, we iteratively solve the convex optimization problem after each training epoch and updating them by using the moving average technique.

For solving the $\boldsymbol{\lambda}$ and $\alpha_t$, we notice that frequently updating these two parameters in the mini-batch level will lead to an instability result during the training. [6] As a consequence, we compute the accumulated confusion matrix, weighted prediction risk, and conditional Wasserstein distance for the whole training epoch and then solve the optimization problem. We use CVXPY to optimize the two standard convex losses. [7]

[6] In the label distribution shift scenarios, the mini-batch datasets are highly labeled imbalanced. If we evaluate $\alpha_t$ over the mini-batch, it can be computationally expensive and unstable.

[7] The optimization problem w.r.t. $\alpha_t$ and $\boldsymbol{\lambda}$ is not large scale, then using the standard convex solver is fast and accurate.

**Algorithm 2** Wasserstein Aggregation Domain Network (unsupervised scenarios, one iteration)

**Require:** Labeled source samples $\hat{\mathcal{S}}_1, \ldots, \hat{\mathcal{S}}_T$, Target samples $\hat{\mathcal{T}}$
**Ensure:** Label distribution ratio $\hat{\alpha}_t$ and task relation simplex $\boldsymbol{\lambda}$. Feature Learner $g$, Classifier $h$, Statistic critic function $d_1, \ldots, d_T$, class centroid for source $\mathbf{C}_t^y$ and target $\mathbf{C}^y$ ($\forall t = [1, T], y \in \mathcal{Y}$).

$\triangleright \triangleright \triangleright$ DNN Parameter Training Stage (fixed $\alpha_t$ and $\boldsymbol{\lambda}$) $\triangleleft \triangleleft \triangleleft$
**for** mini-batch of samples $(\mathbf{x}_{\mathcal{S}_1}, \mathbf{y}_{\mathcal{S}_1}) \sim \hat{\mathcal{S}}_1, \ldots, (\mathbf{x}_{\mathcal{S}_T}, \mathbf{y}_{\mathcal{S}_T}) \sim \hat{\mathcal{S}}_T$, $(\mathbf{x}_{\mathcal{T}}) \sim \hat{\mathcal{T}}$ **do**
  Predict target pseudo-label $\bar{\mathbf{y}}_{\mathcal{T}} = \text{argmax}_y h(g(\mathbf{x}_{\mathcal{T}}), y)$
  Compute source confusion matrix for each batch (un-normalized)
    $C_{\hat{\mathcal{S}}_t} = \#[\text{argmax}_{y'} h(z, y') = y, Y = k]$ $(t = 1, \ldots, T)$
  Compute the *batched* class centroid for source $C_t^y$ and target $C^y$.
  Moving Average for update source/target class centroid: (We set $\epsilon_1 = 0.7$)
    Source class centroid update $\mathbf{C}_t^y = \epsilon_1 \times \mathbf{C}_t^y + (1 - \epsilon_1) \times C_t^y$
    Target class centroid update $\mathbf{C}^y = \epsilon_1 \times \mathbf{C}^y + (1 - \epsilon_1) \times C^y$
  Updating $g, h, d_1, \ldots, d_T$ (SGD and Gradient Reversal), based on Eq.(6)
**end for**
$\triangleright \triangleright \triangleright$ Estimation $\hat{\alpha}_t$ and $\boldsymbol{\lambda}$ $\triangleleft \triangleleft \triangleleft$
Compute the global(normalized) source confusion matrix
$C_{\hat{\mathcal{S}}_t} = \hat{\mathcal{S}}_t[\text{argmax}_{y'} h(z, y') = y, Y = k]$ $(t = 1, \ldots, T)$
Solve $\alpha_t$ (denoted as $\{\alpha_t'\}_{t=1}^T$) by Equation (2) (Or Eq.(5)) in the partial scenario).
Update $\alpha_t$ by moving average: $\alpha_t = 0.8 \times \alpha_t + 0.2 \times \alpha_t'$
Compute the weighted loss and weighted centroid distance, then solve $\boldsymbol{\lambda}$ (denoted as $\boldsymbol{\lambda}'$) from Sec. 2.3.
Updating $\boldsymbol{\lambda}$ by moving average: $\boldsymbol{\lambda} = 0.8 \times \boldsymbol{\lambda} + 0.2 \times \boldsymbol{\lambda}'$

**Algorithm 3** Wasserstein Aggregation Domain Network (Limited Target Data, one iteration)

**Require:** Labeled source samples $\hat{\mathcal{S}}_1, \ldots, \hat{\mathcal{S}}_T$, Target samples $\hat{\mathcal{T}}$, Label shift ratio $\alpha_t$
**Ensure:** Task relation simplex $\boldsymbol{\lambda}$. Feature Learner $g$, Classifier $h$, Statistic critic function $d_1, \ldots, d_T$, class centroid for source $\mathbf{C}_t^y$ and target $\mathbf{C}^y$ ($\forall t = [1, T], y \in \mathcal{Y}$).

$\triangleright \triangleright \triangleright$ DNN Parameter Training Stage (fixed $\boldsymbol{\lambda}$) $\triangleleft \triangleleft \triangleleft$
**for** mini-batch of samples $(\mathbf{x}_{\mathcal{S}_1}, \mathbf{y}_{\mathcal{S}_1}) \sim \hat{\mathcal{S}}_1, \ldots, (\mathbf{x}_{\mathcal{S}_T}, \mathbf{y}_{\mathcal{S}_T}) \sim \hat{\mathcal{S}}_T$, $(\mathbf{x}_{\mathcal{T}}) \sim \hat{\mathcal{T}}$ **do**
  Compute the *batched* class centroid for source $C_t^y$ and target $C^y$.
  Moving Average for update source/target class centroid: (We set $\epsilon_1 = 0.7$)
    Source class centroid update $\mathbf{C}_t^y = \epsilon_1 \times \mathbf{C}_t^y + (1 - \epsilon_1) \times C_t^y$
    Target class centroid update $\mathbf{C}^y = \epsilon_1 \times \mathbf{C}^y + (1 - \epsilon_1) \times C^y$
  Updating $g, h, d_1, \ldots, d_T$ (SGD and Gradient Reversal), based on Eq.(6).
**end for**
$\triangleright \triangleright \triangleright$ Estimation $\boldsymbol{\lambda}$ $\triangleleft \triangleleft \triangleleft$
Solve $\boldsymbol{\lambda}$ by Sec. 2.3. (denoted as $\boldsymbol{\lambda}'$)
Updating $\boldsymbol{\lambda}$ by moving average: $\boldsymbol{\lambda} = 0.8 \times \boldsymbol{\lambda} + 0.2 \times \boldsymbol{\lambda}'$

# L Dataset Description and Experimental Details

## L.1 Amazon Review Dataset

We used the amazon review dataset (Blitzer et al., 2007). It contains four domains (Books, DVD, Electronics, and Kitchen) with positive (label "1") and negative product reviews (label "0"). The data size is 6465 (Books), 5586 (DVD), 7681 (Electronics), and 7945 (Kitchen). We follow the common data pre-processing strategies Chen et al. (2012): use the bag-of-words (BOW) features then extract the top-5000 frequent unigram and bigrams of all the reviews.

We also noticed the original data-set are label balanced $\mathcal{D}(y = 0) = \mathcal{D}(y = 1)$. To enhance the benefits of the proposed approach, we create a new dataset with label distribution drift. Specifically, in the experimental settings, we randomly drop $50\%$ data with label "0" (negative reviews) for all the source data while keeping the target identical, showing in Fig (5).

We choose the MLP model with

- feature representation function $g$: $[5000, 1000]$ units
- Task prediction and domain discriminator function $[1000, 500, 100]$ units,

We choose the dropout rate as $0.7$ in the hidden and input layers. The hyper-parameters are chosen based on cross-validation. The neural network is trained for $50$ epochs and the mini-batch size is 20 per domain. The optimizer is Adadelta with a learning rate of 0.5.

**Experimental Setting** We use the amazon Review dataset for two transfer learning scenarios (limited target labels and unsupervised DA). We first randomly select 2K samples for each domain. Then we create a drifted distribution of each source, making each source $\approx 1500$ and target sample still 2K.

In the unsupervised DA, we use these labeled source tasks and *unlabelled* target task, which aims to predict the labels on the target domain.

In the conventional transfer learning, we random sample only $10\%$ dataset ($\approx 200$ samples) as the target training set and the rest $90\%$ samples as the target test set.

We select $C_0 = 0.01$ and $C_1 = 1$ for these two transfer scenarios. In both practical settings, we set the maximum training epoch as 50.

(a) (b)

Figure 5: Amazon Review dataset (a) Original Label Training Distribution; (b) Label-Shifted distribution with sources tasks: Book, Dvd, Electronic, and target task Kitchen. We randomly drop $50\%$ of the negative reviews for all the source distribution while keeping the target label distribution unchanged.

### L.2 Digit Recognition

We follow the same settings of Ganin et al. (2016) and we use four-digit recognition datasets in the experiments MNIST, USPS, SVHN, and Synth. MNIST and USPS are the standard digits recognition task. Street View House Number (SVHN) Ganin et al. (2016) is the digit recognition dataset from house numbers in Google Street View Images. Synthetic Digits (Synth) Ganin et al. (2016) is a synthetic dataset that by various transforming SVHN dataset.

We also visualize the label distribution in these four datasets. The original datasets show an almost uniform label distribution on the MNIST as well as Synth, (showing in Fig. 7 (a)). In our paper, we generate a label distribution drift on the source datasets for each multi-source transfer learning. Concretely, we drop $50\%$ of the data on digits 5-9 of all the sources while we keep the target label distribution unchanged. (Fig. 7 (b) illustrated one example with sources: Mnist, USPS, SVHN, and Target Synth. We drop the labels only on the sources.)

MNIST and USPS images are resized to $32 \times 32$ and represented as 3-channel color images to match the shape of the other three datasets. Each domain has its own given training and test sets when downloaded. Their respective training sample sizes are 60000, 7219, 73257, 479400, and the respective test sample sizes are 10000, 2017, 26032, 9553.

The model structure is shown in Fig. 6. There is no dropout and the hyperparameters are chosen based on cross-validation. It is trained for 60 epochs and the mini-batch size is 128 per domain. The optimizer is Adadelta with a learning rate of 1.0. We adopted $\gamma = 0.5$ for MDAN and $\gamma = 0.1$ for DARN in the baseline (Wen et al., 2020).

**Experimental Setting** We use the Digits dataset for two transfer learning scenarios (limited target labels and unsupervised DA). Notice the USPS data has only 7219 samples and the digits dataset is relatively simple. We first randomly select 7K samples for each domain. We create a drifted distribution of each source, making each source $\approx 5300$, and the target sample still 7K.

In the unsupervised DA, we use these labeled source tasks and *unlabelled* target task, which aims to predict the labels on the target domain.

In the transfer learning with limited data, we random sample only $10\%$ dataset ($\approx$ 700 samples) as the target training set and the rest $90\%$ samples as the target test set.

We select $C_0 = 0.01$ and $C_1$ as the maximum prediction loss $C_1 = \max_t R^{\alpha_t}(h)$ as the hyper-parameters across these two scenarios. The maximum training epoch is 60.

1. Feature extractor: with 3 convolution layers.
   'layer1': 'conv': [3, 3, 64], 'relu': [], 'maxpool': [2, 2, 0],
   'layer2': 'conv': [3, 3, 128], 'relu': [], 'maxpool': [2, 2, 0],
   'layer3': 'conv': [3, 3, 256], 'relu': [], 'maxpool': [2, 2, 0],
2. Task prediction: with 3 fully connected layers.
   'layer1': 'fc': [*, 512], 'act_fn': 'relu',
   'layer2': 'fc': [512, 100], 'act_fn': 'relu',
   'layer3': 'fc': [100, 10],
3. Domain Discriminator: with 2 fully connected layers.
   *reverse_gradient*()
   'layer1': 'fc': [*, 256], 'act_fn': 'relu',
   'layer2': 'fc': [256, 1],

Figure 6: Neural Network Structure in the digits recognition (Ganin et al., 2016)

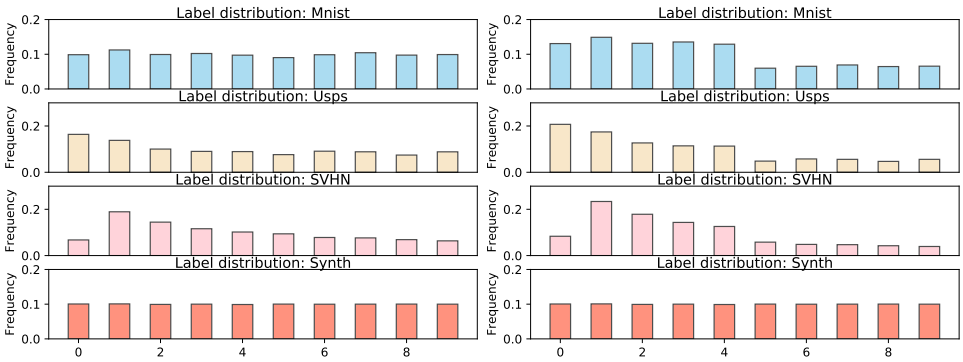


(a) (b)

Figure 7: One example in Digits dataset with Sources: MNIST, USPS, SVHN and Target Synth. We randomly drop $50\%$ data on digits 5-9 in all sources while keeping target label distribution unchanged.

### L.3 Office-Home dataset

To show the dataset in the complex scenarios, we use the challenging Office-Home dataset (Venkateswara et al., 2017). It contains images of 65 objects such as a spoon, sink, mug, and

pen from four different domains: Art (paintings, sketches, and/or artistic depictions), Clipart (clipart images), Product (images without background), and Real-World (regular images captured with a camera). One of the four datasets is chosen as an unlabelled target domain and the other three datasets are used as labeled source domains.

The dataset size is 2427 (Art), 4365 (Clipart), 4439 (Product), 4357 (Real-World). We follow the same training/test procedure as (Wen et al., 2020). We additionally visualize the label distribution $\mathcal{D}(y)$ in four domains in Fig.9, which illustrated the inherent different label distributions. We did not re-sample the source label distribution to uniform distribution in the data pre-processing step. All the baselines are evaluated under the same setting.

We use the ResNet50 (He et al., 2016) pretrained from the ImageNet in PyTorch as the base network for feature learning and put an MLP with the network structure shown in Fig. 10.

**Experimental Settings** We use the original Office-Home dataset for two transfer learning scenarios (unsupervised DA and label-partial unsupervised DA). We use SGD optimizer with learning rate 0.005, momentum 0.9 and weight_decay value 1e-3. It is trained for 100 epochs and the mini-batch size is 32 per domain. As for the baselines, MDAN use $\gamma$ = 1.0 while DARN use $\gamma$ = 0.5. We select $C_0 = 0.01$ and $C_1$ as the maximum prediction loss $C_1 = \max_t R^{\alpha_t}(h)$ as the hyper-parameters across these two scenarios.

In the multi-source unsupervised partial DA, we randomly select 35 classes from the target (by repeating 3 samplings), then at each sampling we run 5 times. The final result is based on these $3 \times 5 = 15$ repetitions.

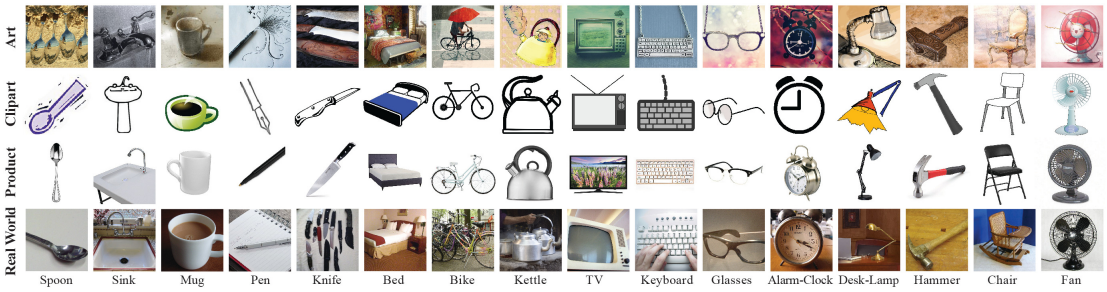


Figure 8: Samples Images From Office-Home dataset (Venkateswara et al., 2017), which consists four domains with non-uniform label distribution.

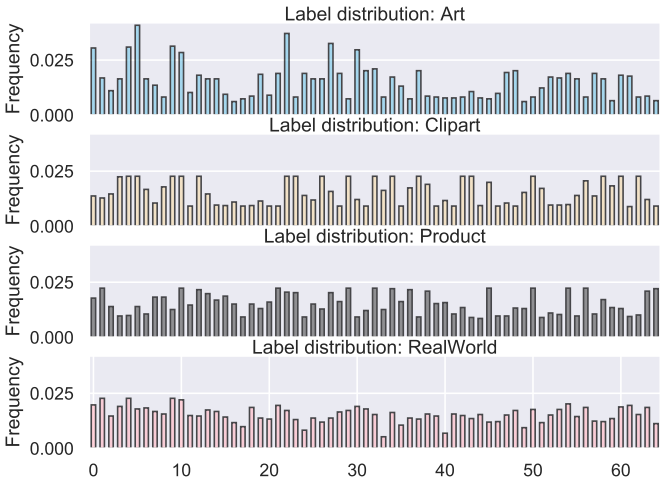


Figure 9: Label distribution of Office-Home Dataset

1. Feature extractor: ResNet50 (He et al., 2016),
2. Task prediction: with 3 fully connected layers.
   'layer1': 'fc': [*, 256], 'batch_normalization', 'act_fn': 'Leaky_relu',
   'layer2': 'fc': [256, 256], 'batch_normalization', 'act_fn': 'Leaky_relu',
   'layer3': 'fc': [256, 65],
3. Domain Discriminator: with 3 fully connected layers.
   *reverse_gradient*()
   'layer1': 'fc': [*, 256], 'batch_normalization', 'act_fn': 'Leaky_relu',
   'layer2': 'fc': [256, 256], 'batch_normalization', 'act_fn': 'Leaky_relu',
   'layer3': 'fc': [256, 1], 'Sigmoid',

Figure 10: Neural Network Structure in the Office-Home

# M ANALYSIS IN UNSUPERVISED DA

## M.1 ABLATION STUDY: DIFFERENT DROPPING RATE

To show the effectiveness of our proposed approach, we change the drop rate of the source domains, showing in Fig.(11). We observe that in task Book, DVD, Electronic, and Kitchen, the results are significantly better under a large label-shift. In the initialization with almost no label shift, the state-of-the-art DARN illustrates a slightly better ($< 1\%$) result.

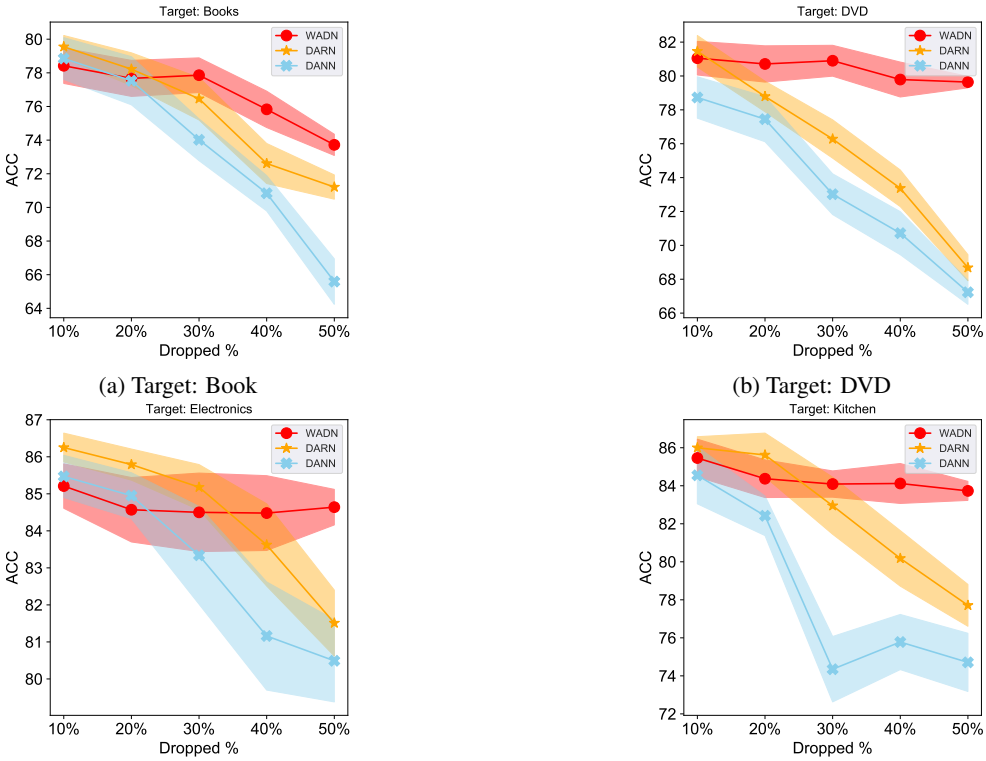


(a) Target: Book (b) Target: DVD

(c) Target: Electronics (d) Target: Kitchen

Figure 11: Different label drift levels on Amazon Dataset. Larger dropping rate means higher label shift.

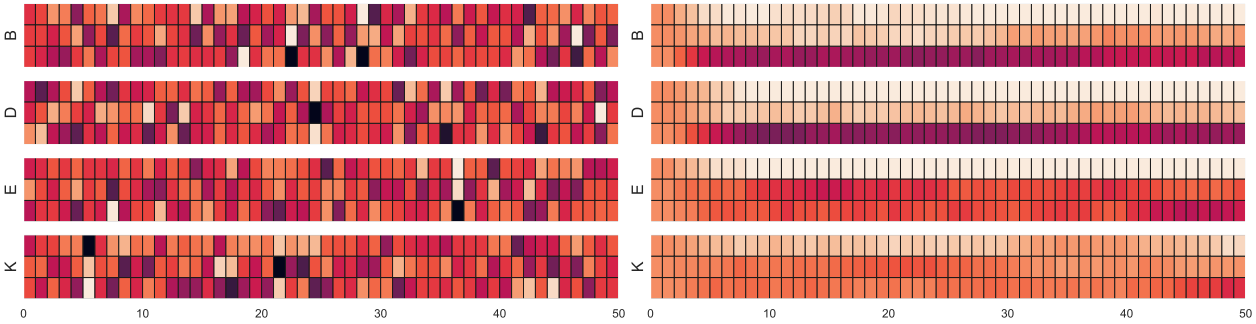


(a) DARN (b) WADN

Figure 12: Source Shifted Amazon Dataset. Evolution of $\boldsymbol{\lambda}$ during the training. B=Books, D=DVD, E=Electronics, K=Kitchen.

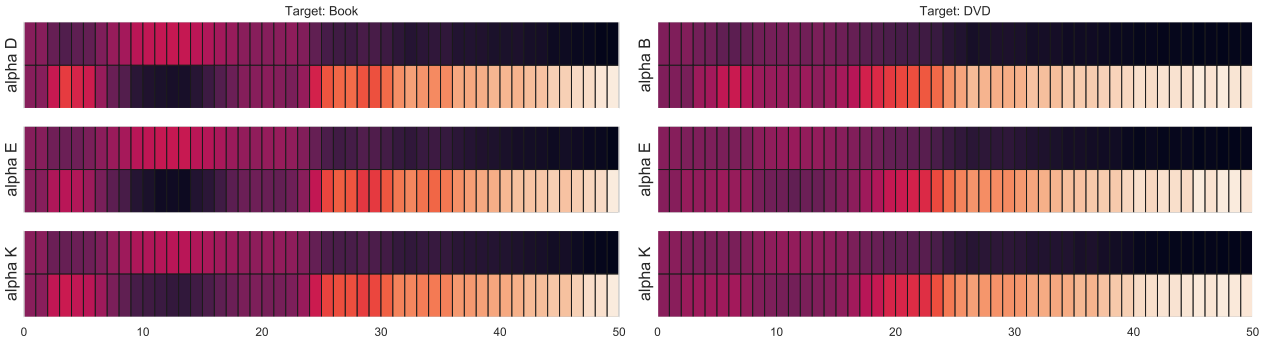


(a) Target: Book (b) Target: DVD

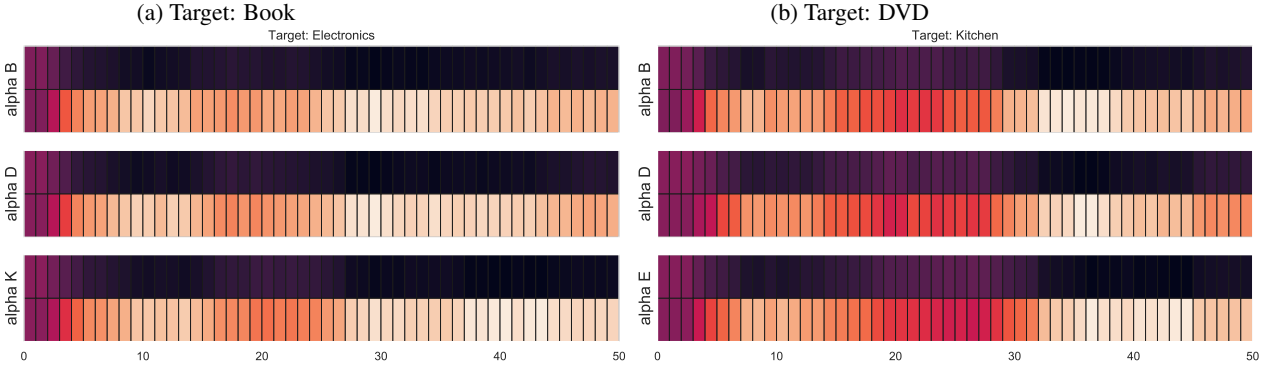


(c) Target: Electronics (d) Target: Kitchen

Figure 13: Amazon Dataset. WADN approach: evolution of $\hat{\alpha}_t$ during the training. Darker indicates higher Value. Since we drop $y = 0$ in the sources, then the true $\alpha_t(0) > 1$ will be assigned with higher value.

### M.2 Additional Analysis on Amazon Dataset

We present two additional results to illustrate the working principles of WADN, showing in Fig. (12) and (13).

We visualize the evolution of $\boldsymbol{\lambda}$ between DARN and WADN, which both used theoretical principled approach to estimate $\boldsymbol{\lambda}$. We observe that in the source shifted data, DARN shows an inconsistent estimator of $\boldsymbol{\lambda}$ Fig. (12). This is different from the observation of Wen et al. (2020). We think it may in the conditional and label distribution shift problem, using $\hat{R}_{\mathcal{S}}(h(z)) + \text{Discrepancy}(\mathcal{S}(z), \mathcal{T}(z))$ to update $\boldsymbol{\lambda}$ is unstable. In contrast, WADN illustrates a relative consistent estimator of $\boldsymbol{\lambda}$ under the source shifted data.

In addition, WARN gradually and correctly estimates the unbalanced source data and assign higher wights $\alpha_t$ for label $y = 0$ (first row of Fig.(13)). These principles in WADN jointly promote significantly better results.

### M.3 Additional Analysis on Digits Dataset

We show the evolution of $\hat{\alpha}_t$ on WADN, which verifies the correctness of our proposed principle. Since we drop digits 5-9 in the source domains, the results in Fig. (14) illustrate a higher $\hat{\alpha}_t$ on these digits.

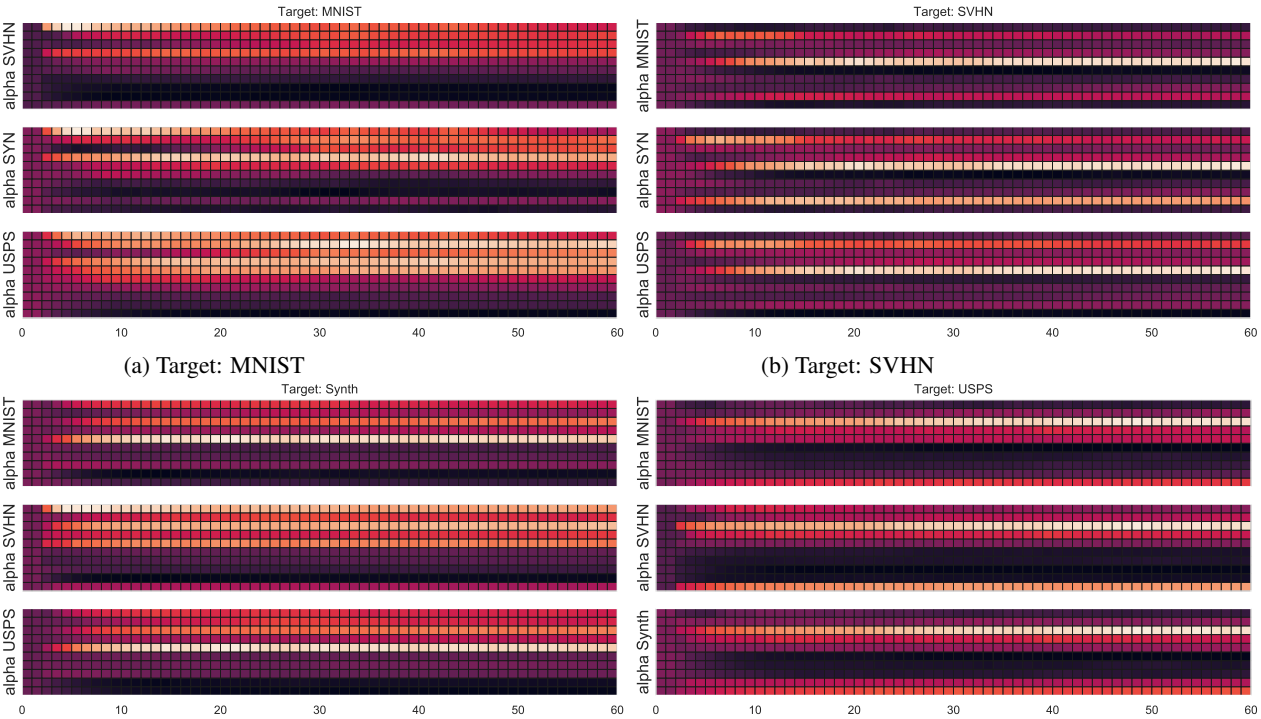


(a) Target: MNIST (b) Target: SVHN

(c) Target: Synth (d) Target: USPS

Figure 14: Digits Dataset. WADN approach: evolution of $\hat{\alpha}_t$ during the training. Darker indicates higher value. Since we drop digits $5-9$ on source domain, therefore, $\alpha_t(y)$, $y \in [5, 9]$ will be assigned with a relative higher value.

## N Partial multi-source Unsupervised DA

From Fig. (15), WADN is consistently better than other baselines, given different selected classes.

Besides, when fewer classes are selected, the accuracy in DANN, PADA, and DARN is not drastically dropping but maintaining a relatively stable result. We think the following possible reasons:

- The reported performances are based on the **average of different selected sub-classes rather than one sub-class selection.** From the statistical perspective, if we take a close look at the **variance**, the results in DANN are *much more unstable* (higher std) inducing by the different samplings. Therefore, the conventional domain adversarial training is improper for handling the partial transfer since it is not reliable and negative transfer still occurs.
- In multi-source DA, it is equally important to detect the non-overlapping classes and find the most similar sources. Comparing the baselines that only focus on one or two principles shows the importance of unified principles in multi-source partial DA.

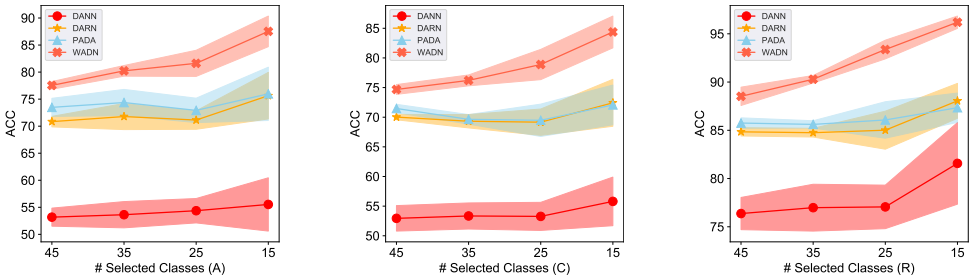


(a) Target: Art (b) Target: Clipart (c) Target: Real-World

Figure 15: Multi-source Label Partial DA: Performance with different target selected classes.

- We also observe that in the Real-World dataset, the DANN improves the performance by a relatively large value. This is due to the inherent difficultly of the learning task itself. In fact, the Real-World domain illustrates a much higher performance compared with other domains. According to the Fano lower bound, *a task with smaller classes is generally easy to learn*. It is possible the vanilla approach showed improvement but still with a much higher variance.

Fig (16), (17) showed the estimated $\hat{\alpha}_t$ with different selected classes. The results validate the correctness of WADN in estimating the label distribution ratio.

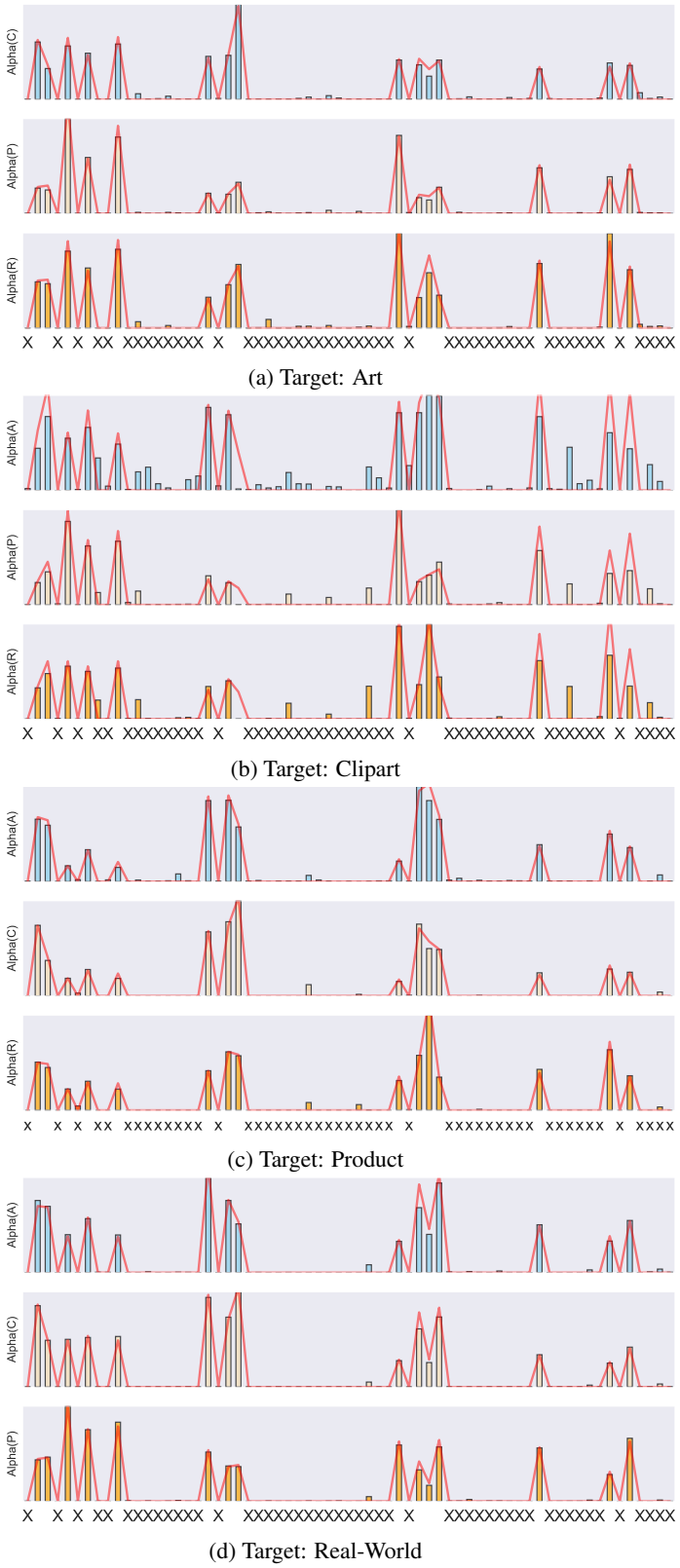


Figure 16: We select 15 classes and visualize estimated $\hat{\alpha}_t$ (the bar plot). The "X" along the x-axis represents the index of **dropped** 50 classes. The red curves are the ground-truth label distribution ratio.

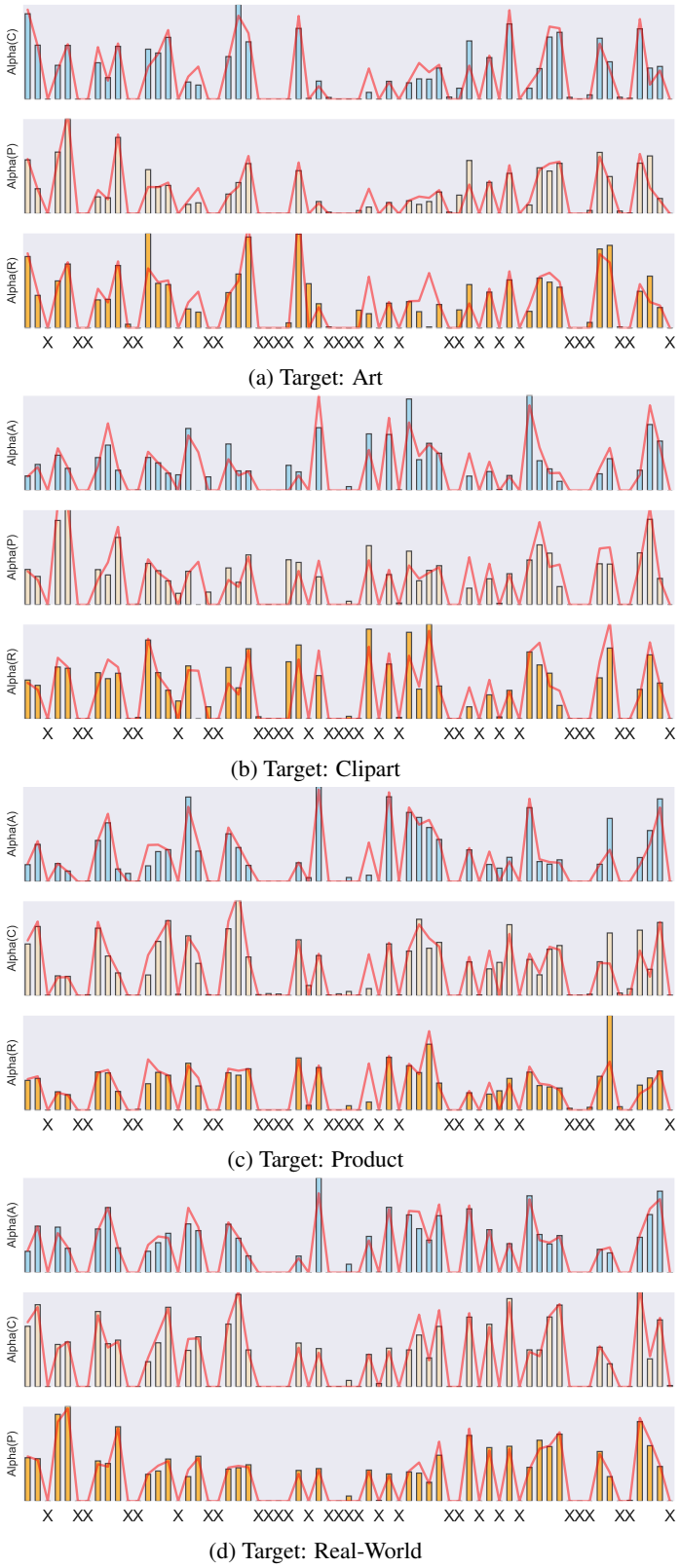


(a) Target: Art

(b) Target: Clipart

(c) Target: Product

(d) Target: Real-World

Figure 17: We select 35 classes and visualize estimated $\hat{\alpha}_t$ (the bar plot). The "X" along the x-axis represents the index of **dropped** 30 classes. The red curves are the ground-truth label distribution ratio.